Abstract

In this chapter, we present the synthesis of new pyrazole based N_4-coorinated tripodal ligand *N*,*N*-bis(3,5-dimethyl-*1H*-pyrazol-1-yl)methyl-N_2-phenylethane-1,2-diamine (bdpab), four mononuclear copper(II) complexes [Cu(bdpab)X]Y and two binuclear cobalt(II) complexes $[Co(bdpab)Cl]_2Y_2$ (X = Cl^-, Br^- ; Y = PF_6^-, BF_4^-) and the compounds were characterized by elemental analyses, IR spectral data, molar conductivity measurement, EPR and crystal structure determination. Single crystal X-ray diffraction studies indicate that the copper centers in the complexes $[Cu(bdpab)Cl]PF_6$ and $[Cu(bdpab)Br]PF_6$ have distorted square pyramidal geometry and cobalt atom in complex $[Co(bdpab)Cl]_2(PF_6)_2$ has octahedral geometry and two $[Co(bdpab)Cl]^+$ units are linked by two (μ-Cl) bridges. Copper(II) complexes form 1D supramolecular chain along c-axis through C-H-π interaction whereas cobalt(II) complex form 1D supramolecular chain along a-axis through π-π interaction. The antimicrobial activity of complexes $[Cu(bdpab)Cl]PF_6$, $[Cu(bdpab)Br]PF_6$ and $[Co(bdpab)Cl]_2(PF_6)_2$ were investigated against gram positive (*Bacillus subtilus, Streptococcus aureus*) and gram negative (*Escherichia coli, Pseudomonas aeruginosa*) bacterial strain by agar well dilution method and have demonstrated significant antimicrobial activity of the compounds and $[Co(bdpab)Cl]_2(PF_6)_2$ has the best antibacterial activity among the synthesized complexes. The studies on the interaction of complexes and DNA by agarose gel electrophoresis method revealed that the complexes can effectively cleave the circular plasmid DNA at very low concentrations. The cytotoxic activity of the complexes against A549 lung cancer cells showed that the complexes have better cytotoxic activity than corresponding metal salts and $[Cu(bdpab)Br]PF_6$ complex has best cytotoxic activity among the synthesized complexes.

4.1. Introduction

Since the discovery of cis-platin as an anti-cancer agent, design and synthesis of new transition metal compounds and their interaction with DNA have been an important area of research in bioinorganic chemistry for the development of new material as the therapeutic agent [1-4]. It is well known that gene has important role in the biological process and the study of the interaction of DNA with transition metal complexes is important for the development of less toxic, target specific and less side effect of the transition metal containing metallodrugs [5-6]. Transition metal complexes are used as bioactive complex because they have different binding ability, coordination numbers and oxidation states etc. Among the transition metal complexes investigated as therapeutic agent, majority are from copper as it is an essential element for the biological system and has low toxicity [8-16]. Since cobalt is also important elements in the bio system, the interaction of cobalt with DNA has been attracted recently [17-18]. Since the DNA and transition metal ions interaction depends on the donor atom of the ligand, nitrogen coordinating ligands such as poly-pyridine are used mostly for the synthesis of bioactive transition metal complexes [19-20]. Many copper(II) and cobalt(II) complexes with tripodal ligands have been investigated for their anticancer properties [21-23]. There are few reports on the bioactivities on the model complexes of bleomycin with imidazole, pyrimidinyl amino and amino donor groups of ligands [24-26], since there are some similarities between the metal binding of model complexes and metal complexes with tripodal pyrazole-based N_4-tetradentate ligands, we are interested to study the bioactivities of the copper(II) and cobalt(II) complexes with this pyrazolyl containing ligand.

In this chapter, we have discussed syntheses and characterization of new mononuclear copper(II) complexes of the type [Cu(bdpad)X]Y and binuclear cobalt(II) complexes of the type $[Co(bdpab)X]_2(Y)_2$ (X = Cl or Br and Y =BF_4 or PF_6) with new N_4-coorinated tripodal ligand *N*,*N*-bis(3,5-dimethyl-*1H*-pyrazol-1-yl)methyl-N_2-phenylethane-1,2-diamine (bdpab). Crystal structures of three complexes [Cu(bdpab)Cl]PF_6, [Cu(bdpab)Br]PF_6 and $[Co(bdpab)Cl]_2(PF_6)_2$ have been solved by single crystal X-ray diffraction method. Antimicrobial activity, cytotoxicity and DNA cleavage study of the complexes have been investigated in detail.

4.2. Experimental

4.2.1. Materials

Materials used for the synthesis of ligand and complexes are discussed in Chapter 2 [section 2.2.1.]. $CuCl_2.2H_2O$, $CuBr_2.4H_2O$ (Loba, India), $CoCl_2.6H_2O$ (Siscochem, India), *N*-phenylethylenediamine (Aldrich) and NH_4BF_4 were reagent grade and used as received.

4.2.2. Physical measurements

Room temperature magnetic susceptibilities of powder samples were measured using a Faraday magnetic balance equipped with a Metler UMX 5 balance, OMEGA temperature controller with a field strength of 0.8 T using Hg $[Co(SCN)_4]$ as the reference. X-band EPR measurements were performed on a Bruker EMX EPR spectrometer at liquid nitrogen temperature (77 K).

4.2.3. Antimicrobial activity assay

The antimicrobial activity of the complexes were determine using various concentrations of Cu(II) and the complexes were prepared in distilled water with not more than 0.1% DMSO to assist dissolution. The screening was carried out using Gram positive (*Bacillus subtilis, Streptococcus aureus*) and Gram negative (*Escherichia Coli, Pseudomonas aeruginosa*) bacterial strains by agar well diffusion method. All the compounds were tested in duplicates. The Luria Bertani (LB) agar plates with 4 mm thickness were spread with 100 µl of overnight cultures. The test compounds at different concentrations were added to the wells (5 mm diameter) made in the agar plates. DMSO at the concentration of 0.1% was used as a negative control and 1 mg/mL of chloramphenicol was used as a positive control for the assay. The plates were incubated at 37˚C for 24 hours. The plates were checked for zones of inhibition after incubation.

4.2.4. Cell line and culture

Human lung carcinoma (A549) cells were procured from National Centre for Cell Science, Pune, India. The cell cultures were grown in Dulbecco's modified Eagle's medium (DMEM, Himedia) supplemented with 10% fetal bovine serum (Gibco-Invitrogen) and 1% antibiotic (Gibco-Invitrogen). Cell lines were maintained

at 37°C in a 5% (v/v) CO_2 atmosphere with 95% (v/v) humidity in a humidified incubator (Thermo Scientific). Cultures were passaged weekly using trypsin–EDTA (Himedia india) to detach the cells from their culture flasks. The copper(II) and cobalt(II) salts and their complexes were dissolved in DMSO and diluted to the required concentration with culture medium. The DMSO content in the final concentrations did not exceed 0.1%.

4.2.5. Cell Proliferation assay (MTT)

Cell proliferation assay was performed to check the in vitro anticancer activities of the two copper(II) and cobalt(II) salts and their complexes against A549 lung cancer cell line [27]. The cells were seeded in 96-well microplates at a concentration of 5 x 10^4 cells/well. In the 24th hour, the fresh media modified with different concentrations of the test compounds was added. Each concentration was applied in triplicates. Samples of cells grown in non-modified medium served as control. After 24h incubation, the solutions were removed from the plates and (3-(4,5-dimethylthiazol-2-yl)-2,5-diphenyltetrazolium bromide) (MTT) (5 mg/mL DMEM) solution was added followed by 3 h incubation. Medium with MTT was flicked off and the formazan crystals were solubilized in 100 µl DMSO. The absorbance of each well was measured at 540/620 nm by ELISA microplate reader (Thermo Scientific). Relative cell viability, expressed as a percentage of the untreated control (100% viability), was calculated for each concentration. Concentration-response curves were constructed for each experiment. The data are presented as means $\pm$ standard error of the mean. The IC_{50} values were calculated from the curves constructed by plotting cell survival (%) vs the complexes concentration (µg/mL). Statistical differences between control and treated cells at different concentrations were assessed by 2-way anova test in Graph-Pad Prism 5.0 software package.

4.2.6. Cleavage experiment

The bacterial plasmid pBS KS (+) was isolated from *Escherichia coli* strain by alkaline lysis method [28]. The ratio 260 to 280nm (A260/A280) absorbance was checked to be ~1.86, which indicated that the DNA is sufficiently free from protein [29]. The concentration of DNA was determined spectrophotometrically (UV 1601 UV-Visible spectrophotometer, SHIMADZU) at 260 nm using the known molar extinction coefficient value of 6700 M^{-1} cm^{-1} [30]. The DNA was stored at -20º C

until used. Visualization of DNA under UV was done using Alpha imager HP System, Alpha innotech.

The Cu(II) complexes **1**, **3** and **5** were examined for their ability to cleave DNA. For this 3 µM pBS KS(+) plasmid DNA was treated with Cu(II) complexes at various concentration ranging from 10 µM-50 µM along with the addition of 5 µM hydrogen peroxide. A plasmid with volume made up with sterile distilled water was kept as an untreated control. A reaction with 5 µM H_2O_2 alone and with 50µM of the complexes alone were also kept to check their individual effect on the plasmid. After overnight incubation at 37˚C, 5 µl from each reaction was loaded using bromophenol blue (0.25%) and glycerol (30%) loading dye onto 0.8% agarose gel containing ethidium bromide (final 0.5 µg/ml). The gel was observed under UV trans illuminator at 360 nm.

4.2.7. Synthesis of ligand

4.2.7.1. Synthesis of *N*,*N*-bis(3,5-dimethyl-1H-pyrazol-1-yl)methyl-N_2-phenylethane-1,2-diamine (bdpab)

A solution of *N*-(3,5-dimethyl-1H-pyrazole-1-yl)methanol (0.252 g, 2 mmol) in acetonitrile (20 ml) was added to a stirred solution of N-(2-aminoethyl)benzenamine (0.136 g, 1 mmol) in acetonitrile (20 ml) at room temperature and stirring was continued for three days. The resulting solution was then dried over anhydrous Na_2SO_4 and solvent was removed on a vacuum rotary evaporator. A light-yellow viscous liquid was obtained. Purity of the compound was checked by TLC.

Yield. 0.290 g (82%). Found C = 67.97, H = 8.05, N = 23.98%, Elemental analysis Calc. for $C_{20}H_{28}N_6$: C = 68.15, H = 8.01, N = 23.84%. IR (neat) cm^{-1}: ν(-NH), 3200 m; ν(C = C), 1583 s; ν(C = C) + ν (C = N)/pz ring, 1553s, 1467 s; ^{1}H NMR (400 MHz, $CDCl_3$, 20°C), *δ*/ppm: 2.240-2.326 (s, 12H, 4 -CH_3 of pz), 3.142-3.174 (t, J_{HZ} = 6.4 Hz, 2H,-NH-CH_2-CH_2 of ethylene), 3.376-3.392 (t, J_{HZ} = 6.4 Hz, 2H,-NH-CH_2-CH_2 of ethylene), 4.2 (s, 2H, N-CH_2-N), 4.921 (s, 2H, N-CH_2-N), 5.843 (s, 1H, pz ring), 5.853 (s, 1H, pz ring), 6.517 (d, 2H, J_{HZ} = 7.6 Hz, phenyl ring), 6.723 (t, 1H, J_{HZ} = 7.2 Hz, phenyl ring), 7.213-7.256 (m, 2H, phenyl ring). MS (EI): m/z = 353 $(C_{20}H_{28}N_6)^+$, 161 $(C_{10}H_{13}N_2)^+$, 109 $(C_6H_9N_2)^+$, 77 $(C_6H_6)^+$.

4.2.8. Syntheses of complexes

4.2.8.1. Synthesis of [Cu(bdpab)Cl]PF_6 (1)

A solution of ligand bdpab (0.176 g, 0.5 mmol) in methanol (10 ml) was added drop by drop to a stirred light green solution of $CuCl_2.2H_2O$ (0.085 g, 0.5 mmol) in the same solvent (10 ml) and the color changed to dark green immediately. After 10 min, NH_4PF_6 (0.082 g, 0.5 mmol) in methanol (10 ml) was added drop by drop and resulting green color solution was stirred for another 3 h at room temperature, filtered and kept the filtrate for slow evaporation at room temperature. Light green color single crystals were obtained after 5days.

Yield. 0.110 g (74 %). Found C = 40.78, H = 4.88, N = 14.21%. Anal calc for $C_{20}H_{28}ClCuF_6N_6P$: C = 40.47, H = 4.73, N = 14.09%. IR (KBr pellet) cm^{-1}: ν(-NH), 3329 vs; ν(C = C)/ph ring, 1600 s; ν(C = C) + ν (C = N)/pz ring 1551 s, 1474 s; ν(PF_6^-), 848 s. UV-Vis spectra: λ_{max}/nm (ε_{max}/$mol^{-1}cm^{-1}$). 648 (171), 279 (4568), 226 (18067). Λ_M ($\Omega^{-1}cm^2\ mol^{-1}$) = 120. μ_{eff} = 1.76 BM.

4.2.8.2. Synthesis of [Cu(bdpab)Cl]BF_4 (2)

This complex was prepared by following the same procedure as that of complex **1** except NH_4BF_6 was used in place of NH_4PF_6.

Yield. 0.105 g (77%). Found C = 44.77, H = 5.32, N = 15.78%, Anal calc for $C_{20}H_{28}ClCuF_4N_6B$: C = 44.63, H = 5.24, N = 15.61%. IR (KBr pellet) cm^{-1}: ν(-NH), 3132vs; ν(C = C)/ph ring, 1600 s; ν(C = C) + ν (C = N)/pz ring, 1555 s, 1476 s; ν(BF_4^-), 1055br. UV-Vis spectra: λ_{max}/nm (ε_{max}/$mol^{-1}cm^{-1}$). 706 (202), 274 (4695), 220 (15550). Λ_M ($\Omega^{-1}cm^2\ mol^{-1}$) = 120. μ_{eff} = 1.78 BM.

4.2.8.3. Synthesis of [Cu(bdpab)Br]PF_6 (3)

This complex was prepared by following the same procedure as that of complex **1** except $CuBr_2.2H_2O$ was used in place of $CuCl_2.2H_2O$.

Yield. 0.136 g (85%). Found C = 37.20, H = 4.28, N = 13.03%. Anal calc for $C_{20}H_{28}BrCuF_6N_6P$: C = 37.48, H = 4.40, N = 13.11%. IR (KBr pellet) cm^{-1}: ν(-NH), 3242 vs; ν(C = C)/ph ring, 1603 s; ν(C = C) + ν (C = N)/pz ring 1558 s, 1476 s, ν(PF_6^-), 839 s. UV-Vis spectra: λ_{max}/nm (ε_{max}/$mol^{-1}cm^{-1}$). 670 (302), 303 (4241), 225 (19673). Λ_M ($\Omega^{-1}cm^2\ mol^{-1}$) = 120. μ_{eff} = 1.71.

4.2.8.4. Synthesis of [Cu(bdpab)Br]BF_4 (4)

This complex was prepared by following the same procedure as that of complex **1** except $CuBr_2.2H_2O$ and NH_4BF_4 was used in place of $CuCl_2.2H_2O$ and NH_4PF_6.

Yield. 0.117 g (80%). Found C = 41.58, H = 4.72, N = 14.35%. Anal calc for $C_{20}H_{28}BrCuF_4N_6B$: C = 41.22, H = 4.84, N = 14.42%. IR (KBr pellet) cm^{-1}: ν(-NH), 3326 vs; ν(C = C)/ph ring, 1633 s; ν(C = C) + ν (C = N)/pz ring, 1553 s, 1470 s; ν(BF_4^-), 1042 br. UV-Vis spectra: λ_{max}/nm (ε_{max}/$mol^{-1}cm^{-1}$). 709 (237), 301 (3724), 221 (20200). Λ_M ($\Omega^{-1}cm^2\ mol^{-1}$) = 120. μ_{eff} = 1.73.

4.2.8.5. Synthesis of $[Co(bdpab)Cl]_2(PF_6)_2$ (5)

Ligand bdpab (0.176 g, 0.5 mmol) in methanol (10 ml) was added drop by drop to a stirring solution of $CoCl_2.6H_2O$ (0.120 g, 0.5 mmol) in the same solvent (10 ml) and the color changed from light pink to light blue. After 10 min, NH_4PF_6 (0.082 g, 0.5 mmol) in methanol (10 ml) was added drop by drop in the solution. The resulting light blue color solution was stirred for further 3 h at room temperature, filtered and filtrate was kept for slow evaporation. Light pink color single crystals were obtained after one week.

Yield. 0.077 g (52%). Found C = 40.72, H = 4.86, N = 14.18%. Anal calc for $C_{40}H_{56}Cl_2Co_2F_{12}N_{12}P_2$: C = 40.59, H = 4.77, N = 14.02%. IR (KBr Pellet) cm^{-1}: ν(-NH), 3197 vs; ν(C = C)/ph ring, 1603 s; ν(C = C) + ν (C = N)/pz ring 1556 s, 1476 s, ν(PF_6^-), 840 s. UV-Vis spectra: λ_{max}/nm (ε_{max}/$mol^{-1}cm^{-1}$). 830 (54), 628 (207), 607(349), 531 (234), 501 (271), 245 (17259), 200 (32821). Λ_M ($\Omega^{-1}cm^2\ mol^{-1}$) = 120. μ_{eff} = 4.37.

4.2.8.6. Synthesis of $[Co(bdpab)Cl]_2(BF_4)_2$ (6)

This complex was prepared by following the same procedure as that of complex **5** except NH_4BF_6 was used in place of NH_4PF_6.

Yield. 0.081 g (60%). Found C = 45.35, H = 5.37, N = 15.64%. Anal calc for $C_{40}H_{56}Cl_2Co_2F_8N_{12}B_2$: C = 45.01, H = 5.29, N = 15.75%. IR (KBr pellet) cm^{-1}: ν(-NH), 3197 vs; ν(C = C)/ph ring, 1603 s; ν(C = C) + ν (C = N)/pz ring 1556 s, 1476 s; ν(PF_6^-), 840 s. UV-Vis spectra: λ_{max}/nm (ε_{max}/$mol^{-1}cm^{-1}$). 829 (33), 632 (109), 605

(274), 530 (182), 501 (201), 290 (5669), 246 (26217). Λ_M ($\Omega^{-1}cm^2$ mol^{-1}) = 122.μ_{eff} = 4.46.

4.3. Crystal structure determination.

The details of crystal structure determination, data collection, crystal data and some important features of the refinements parameters for complex **1, 3** and **5** are listed in Table 4.1 and selected bond lengths and angles are given in Table 4.2. Crystals of suitable size were obtained by slow evaporation of methanol solution of the compounds. Data were collected with Mo-K_α radiation (λ = 0.71073Å) (graphite monochromator) for all complexes at 110 K on an Oxford X-CALIBUR-S diffractometer equipped with a CCD area detector. The intensity data were collected using ω and φ scans with frame width of 0.5º. The data interpretations were processed with CrysAlisPro, Agilent Technologies, Version 1.171.35.19 [31] and an absorption correction based on the multi-scan method was applied [32]. The reported structures were solved by direct methods and refined by full-matrix least-squares based on F^2 technique using the SHELXL-97 program package [33]. All calculations were carried out using WinGX system Ver-1.64 [34]. All non-hydrogen atoms were refined anisotropically. The positions of the hydrogen atoms were calculated from the difference Fourier map, placed in the calculated positions and constrained to ride on their parent atoms. ORTEP3 for Windows program were used for generating the structures [35].

Table 4.1. Crystallographic parameters of the complexes **1**, **3** and **5.**

	[Cu(bdpab)Cl]PF_6 (1)	**[Cu(bdpab)Br]PF_6 (3)**	**[Co(bdpab)Cl]$_2$(PF_6)$_2$ (5)**
Empirical formula	$C_{20}H_{28}ClCuF_6N_6P$	$C_{20}H_{28}BrCuF_6N_6P$	$C_{40}H_{56}Cl_2Co_2F_{12}N_{12}P_2$
Formula weight	596.44	640.90	1183.67
Temperature (K)	110(10)	110(2)	110(15)
Wavelength (Å)	0.71073	0.71073	0.71073
Crystal system	triclinic	triclinic	triclinic
Space group	*P-1*	*P-1*	*P-1*
a (Å)	9.9493(7)	10.1081(3)	9.6899(3)
b (Å)	10.2231(6)	10.1360(3)	10.8074(5)
c (Å)	13.0782(7)	13.1339(3)	13.1823(5)
α(°)	103.917(5)	106.148(2)	103.944(3)
β(°)	106.243(5)	103.355(2)	102.545(3)
γ(°)	101.402(5)	101.043(2)	105.951(3)
Volume (Å^3)	1188.47(13)	1209.58(6)	1227.36(9)
Z	2	2	1
Density (Mg/m^3)	1.667	1.760	1.6013

Absorption coefficient (μ/mm^{-1})	1.168	2.689	0.941
F(000)	610.0	646.0	606.0
Crystal size (mm)	0.25 x 0.17 x 0.12	0.25 x 0.17 x 0.12	0.28 x 0.18 x 0.14
Theta range for data collection (°)	6.14 to 57.9	6.24 to 58.16	6.44 to 58.02
Index ranges	$-13 \leq h \leq 12$, $-13 \leq k \leq 12$, $-16 \leq l \leq 17$	$-13 \leq h \leq 13$, $-12 \leq k \leq 13$, $-17 \leq l \leq 17$	$-13 \leq h \leq 13$, $-14 \leq k \leq 14$, $-17 \leq l \leq 17$
Reflections collected	10336	26896	26806
Independent reflections	6298 [R(int) = 0.0232]	6482 [R(int) = 0.0363]	6527 [R(int) = 0.0472]
Data / restraints / parameters	6298/0/320	6482/0/320	6527/0/323
Goodness-of-fit on F^2	1.050	1.051	0.906
Final R indices [I>2sigma(I)]	*R1* = 0.0447, *wR2* = 0.1094	*R1* = 0.0352, *wR2* = 0.0857	*R1* = 0.0387, *wR2* = 0.1164
R indices (all data)	*R1* = 0.0553, *wR2* = 0.1151	*R1* = 0.0419, *wR2* = 0.0891	*R1* = 0.0495, *wR2* = 0.1244
Largest diff. peak and hole (eA^{-3})	0.80 and -0.66	0.73 and -0.69	0.74 and -0.87
CCDC	1529402	1529364	1529365

4.4. Results and discussion

4.4.1. Syntheses

The ligand *N*,*N*-bis(3,5-dimethyl-*1H*-pyrazol-1-yl)methyl-N_2-phenylethane-1,2-diamine (bdpab) was synthesized as light yellow viscous liquid by stirring N-(2-aminoethyl)benzenamine and (3,5-dimethyl-*1H*-pyrazole-1-yl)methanol using appropriate mole ratio in dry acetonitrile at room temperature for three days [scheme 4.1]. Purity of the ligand was checked by TLC. The ligand is a new tetradentate chelating molecule and possesses four nitrogen donor sites- two nitrogen donor atoms from the two pyrazole rings, one nitrogen atom from tertiary amine and another from secondary amine. The ligand was characterized by IR, ^{1}H NMR and mass spectrum analyses.

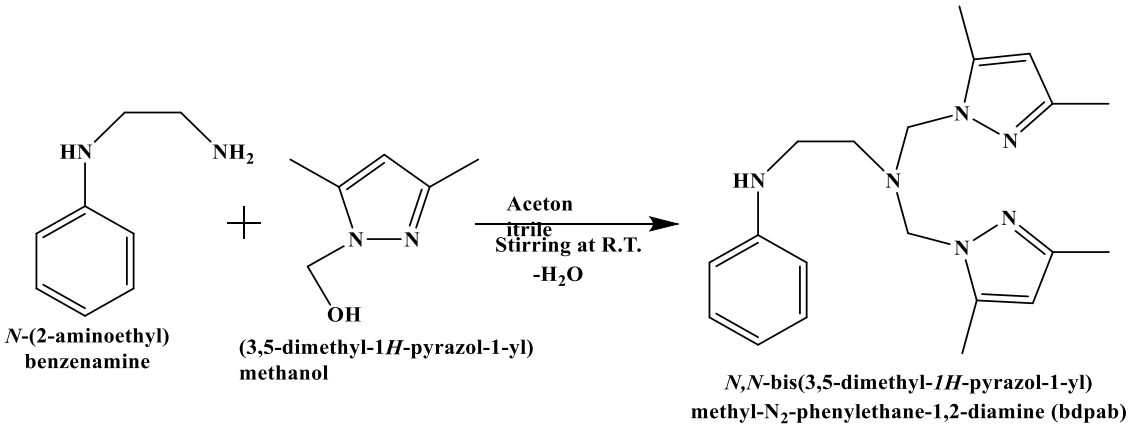

Scheme 4.1. Synthesis of ligand *N*,*N*-bis(3,5-dimethyl-*1H*-pyrazol-1-yl)methyl-N_2-phenylethane-1,2-diamine **(bdpab)**

Four mononuclear five coordinated copper(II) complexes [Cu(bdpab)X]Y and two binuclear six coordinate Co(II) complexes $[Co_2(bdpab)_2(\mu\text{-}Cl)_2]Y_2$ (where, X = Cl^-, Br^- and Y = PF_6^-, BF_4^-) were synthesized through one-pot reaction of metal halides, ligand bdpab and NH_4PF_6/NH_4BF_4 in the 1:1:1 mole ratio respectively, in methanol at room temperature [scheme 4.2]. All the complexes were obtained in good yield and characterized by elemental analysis, UV-Vis, IR, EPR and single crystal X-ray diffraction studies. The ligand bdpab is tetradentate and has utilized its all four nitrogen donor atoms for coordination with metal ions. The coordination of ligand bdpab was confirmed by IR and single crystal X-ray diffraction studies (Fig.4.13(a), 4.14(a) and 4.15(a)). Suitable crystal of complexes **1**, **3** and **5** were obtained by slow

evaporation of solvent at room temperature. Single crystal X-ray data revealed that all copper(II) complexes are mono nuclear five coordinated with distorted square pyramidal geometry whereas cobalt(II)complexes are binuclear with distorted octahedral geometry. Molar conductivity data in CH_3CN solution show all the complexes have 1:1 electrolyte (Λ_M = 120 $\Omega^{-1}cm^2mol^{-1}$) which support the presence of counter anion outside the coordination sphere [36]. All complexes are air stable and soluble in organic solvent like methanol, ethanol, acetonitrile etc.

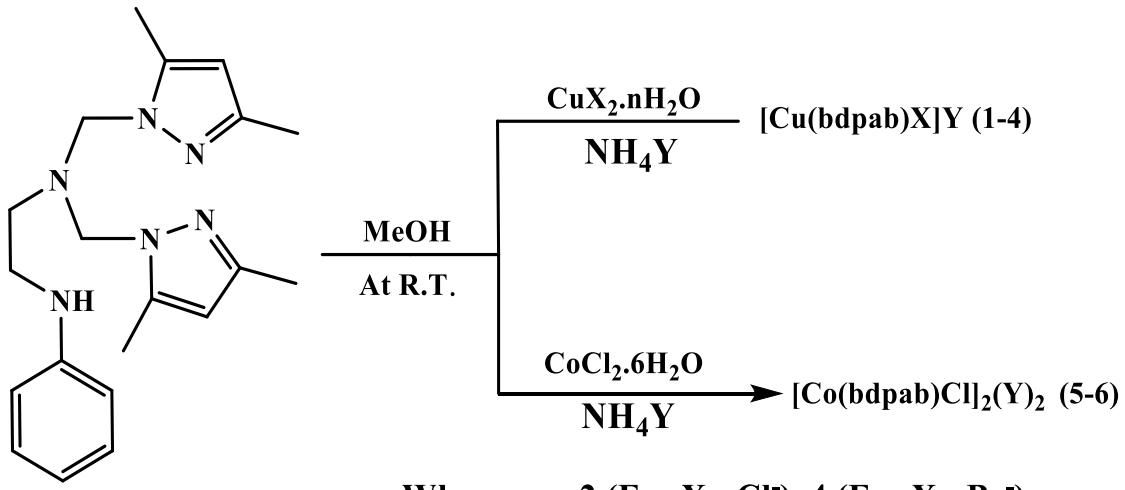

Scheme 4.2. Synthesis of complexes.

4.4.2. Spectral Data

4.4.2.1. ^{1}H NMR and Mass spectral data.

The ^{1}H NMR spectrum of ligand bdpab shows peak at 2.240 - 2.326 δ ppm which confirm the presence of four methyl group of pyrazole ring. The two triplets appear in the region at 3.142-3.174 and 3.376-3.408 δ ppm confirms the presence of -CH_2-CH_2- group of ethylenediamine moiety. Two singlets appear at 4.20 δ ppm and 4.921 δ ppm confirms the presence of two -CH_2- which are connected with pyrazole and ethylenediamine moiety. The aromatic protons of two pyrazole ring appeared at 5.843 and 5.853 δ ppm as singlet. The aromatic protons of phenyl ring appeared at 6.498-7.256 ppm and shows multiplet at 7.213-7.256 δ ppm due to meta hydrogen, triplet at 6.723 δ ppm due to para hydrogen and doublet at 6.517 δ ppm due to ortho hydrogen. Mass spectra of the ligand bdpab shows m/z = 353 $(C_{20}H_{28}N_6)^+$ which corresponds to the mass of the ligand.

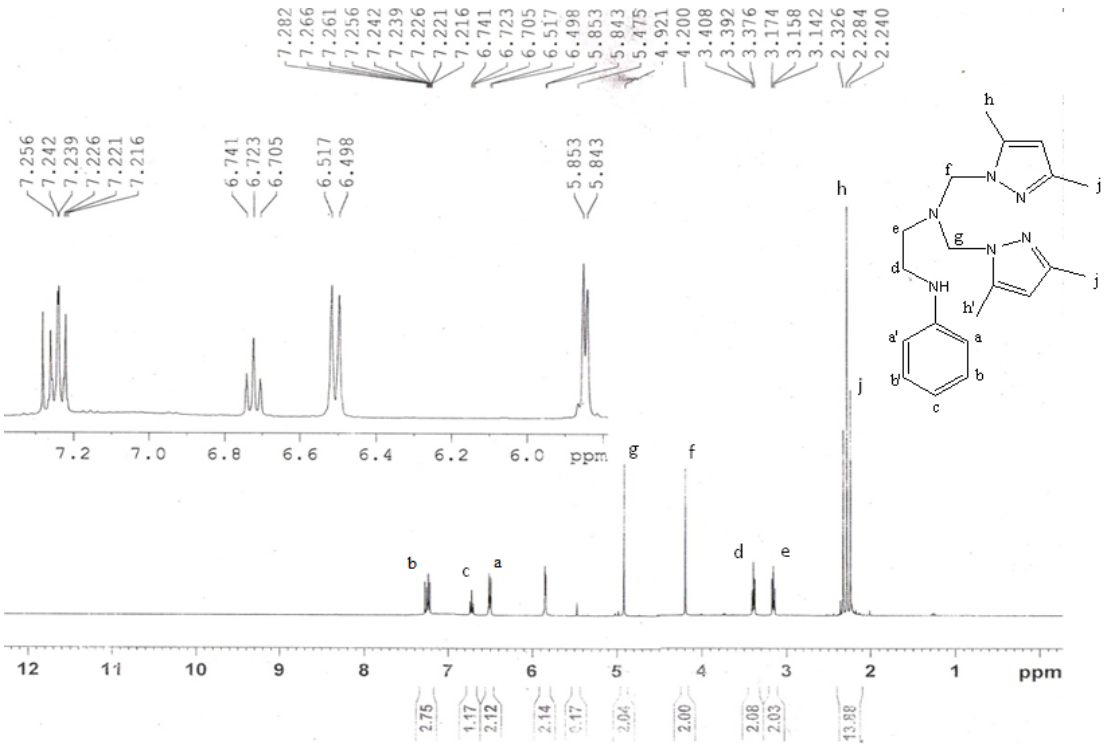

Fig.4.1. ^{1}H-NMR spectrum of *N*,*N*-bis(3,5-dimethyl-1H-pyrazol-1-yl)methyl-N_2-phenylethane-1,2-diamine (bdpab).

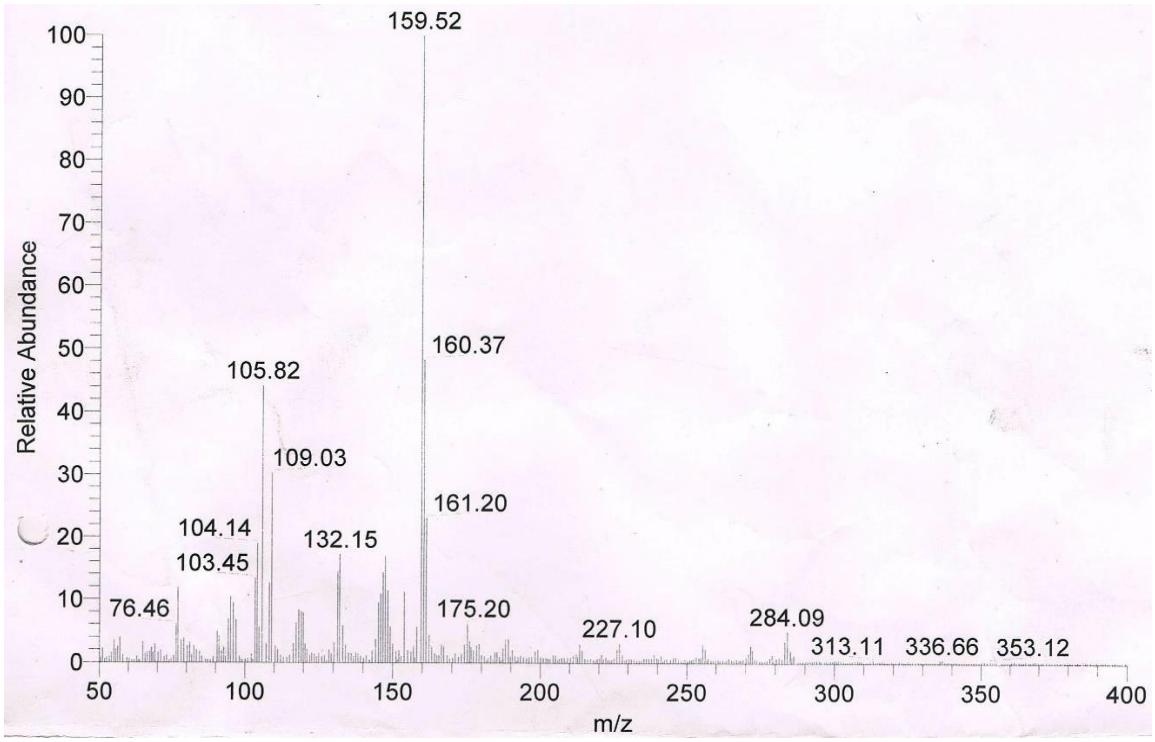

Fig.4.2. Mass spectrum of *N*,*N*-bis(3,5-dimethyl-1H-pyrazol-1-yl)methyl-N_2-phenylethane-1,2-diamine (bdpab).

4.4.2.2. IR spectra

IR spectra data of the ligand exhibits a medium intensity band at 3200 cm^{-1} due to ν(-NH) and two strong bands at 1553 and 1467 cm^{-1} which are assigned as ν(C=C) and ν(C=N) of pyrazolyl group. All complexes exhibit one medium intensity band at ~ 3200 cm^{-1} due to secondary amine(-NH) group and two medium intensity bands at ~ 1553 and ~ 1464 cm^{-1} were due to pyrazolyl ν(C = C) + ν (C = N) group of the ligand (bdpab) and these bands are also present in the IR spectra of ligand with the little difference in frequency indicating the coordination of the ligand to the metal centers. IR spectra of the complexes **1**, **3** and **5** show an intense band at ~ 845 cm^{-1} confirming the presence of ν(PF_6^-) counter anion and complexes **2**, **4** and **6** exhibited a broad band at ~1065 cm^{-1} it indicating the presence of ν(BF_4^-) counter anion [37].

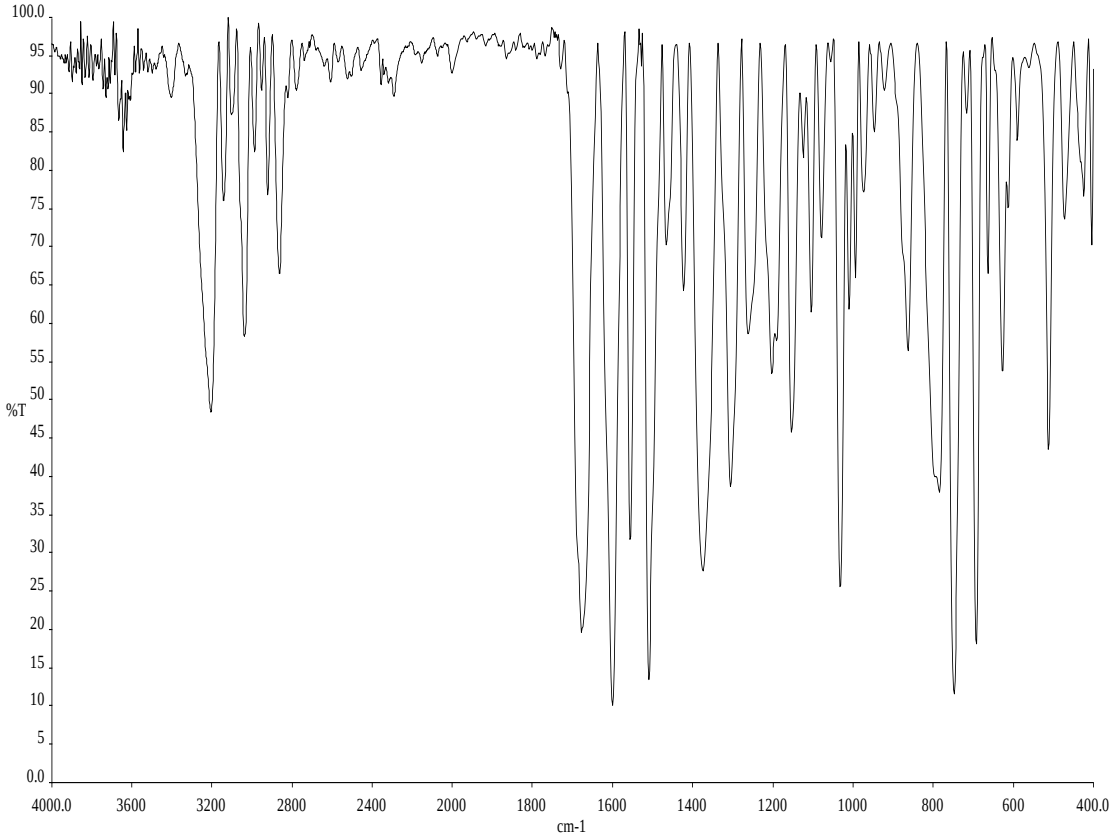

Fig.4.3. IR spectrum of ligand *N*-benzyl-*N*,*N*-bis(3, 5-dimethyl-1*H*- pyrazol-1-yl)-2-methy]-1,2-ethylenediamine (bdpab).

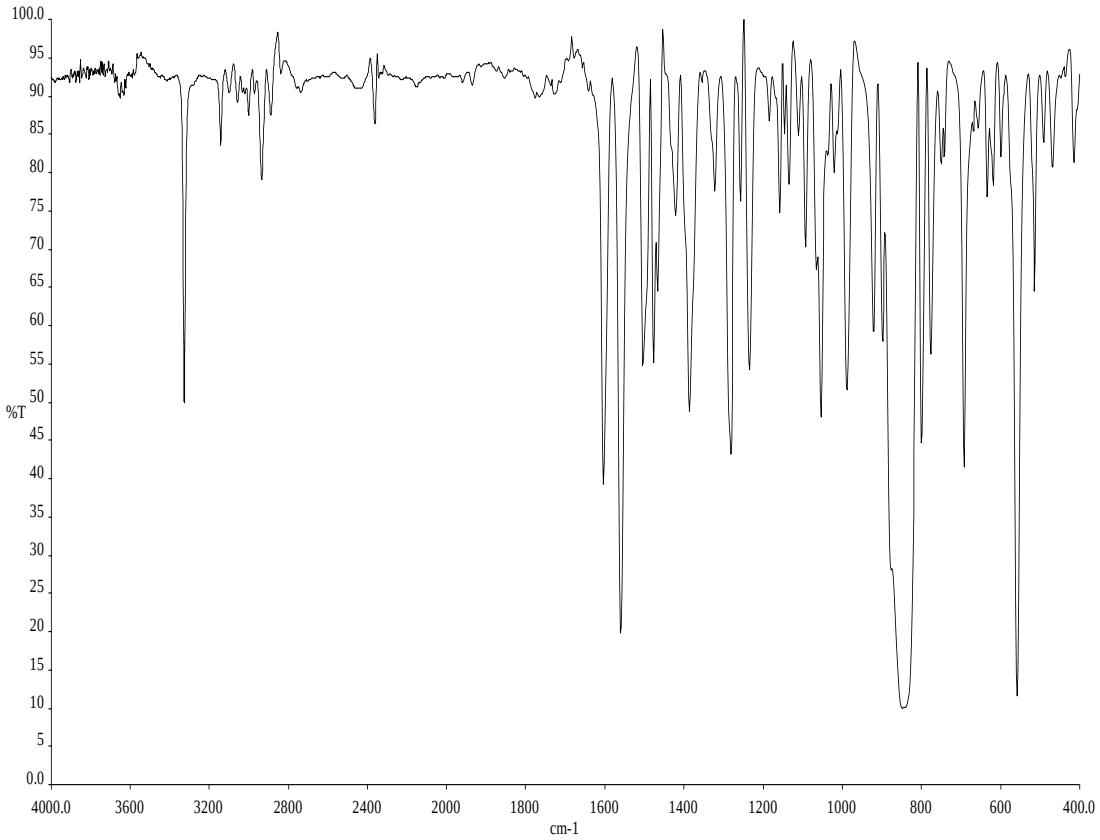

Fig.4.4. IR spectrum of [Cu(bdpab)Cl]PF_6 (**1**).

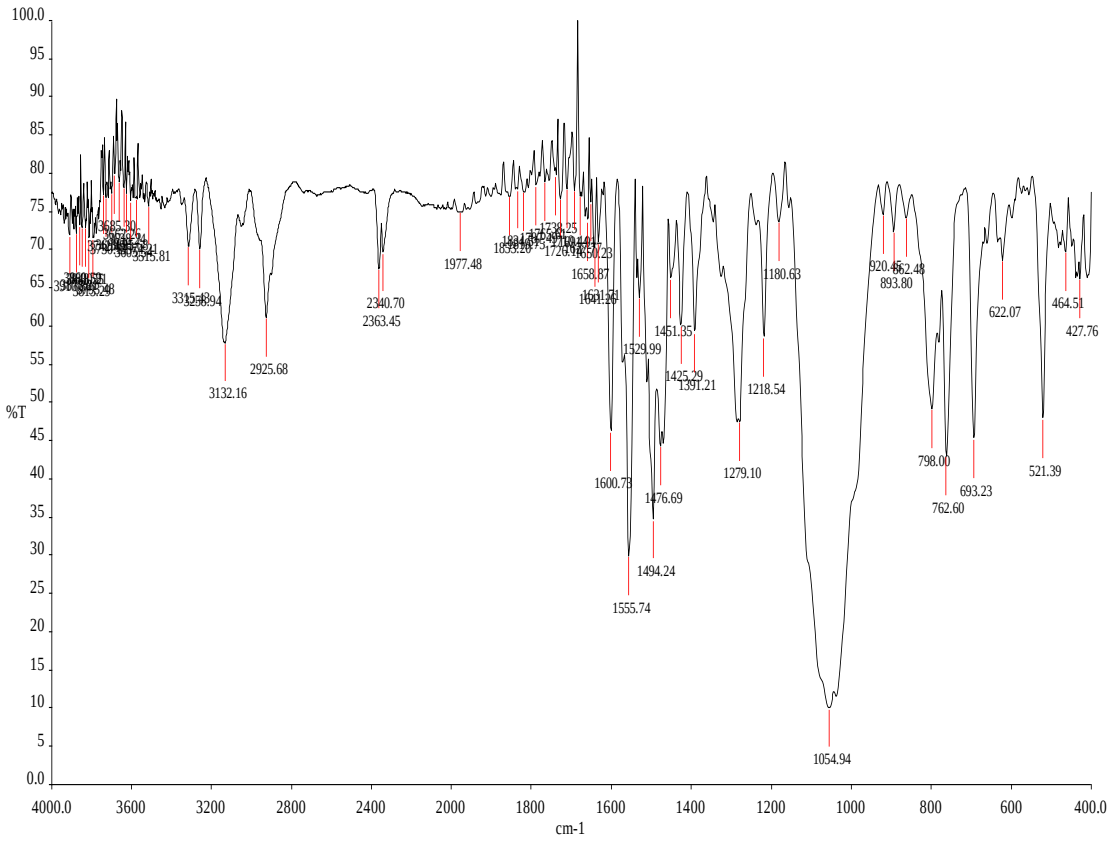

Fig.4.5. IR spectrum of [Cu(bdpab)Cl]BF_4 (**2**).

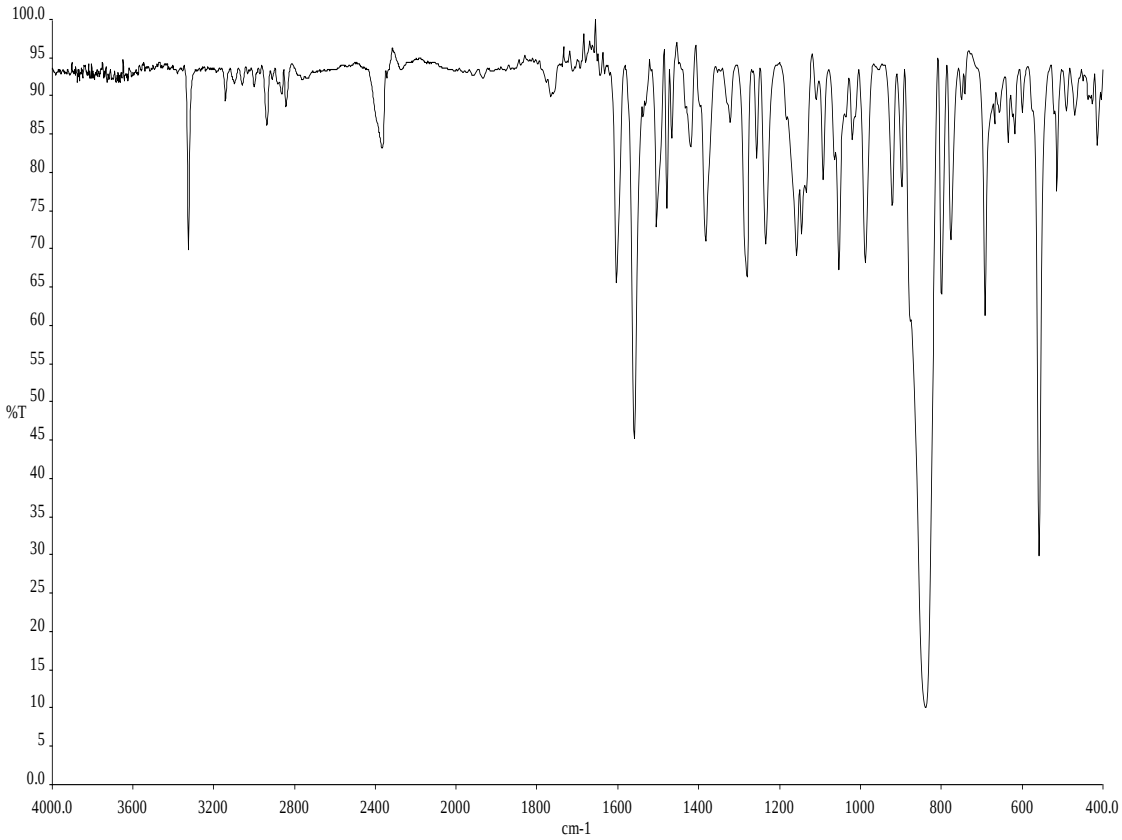

Fig.4.6. IR spectrum of [Cu(bdpab)Br]PF_6 (**3**).

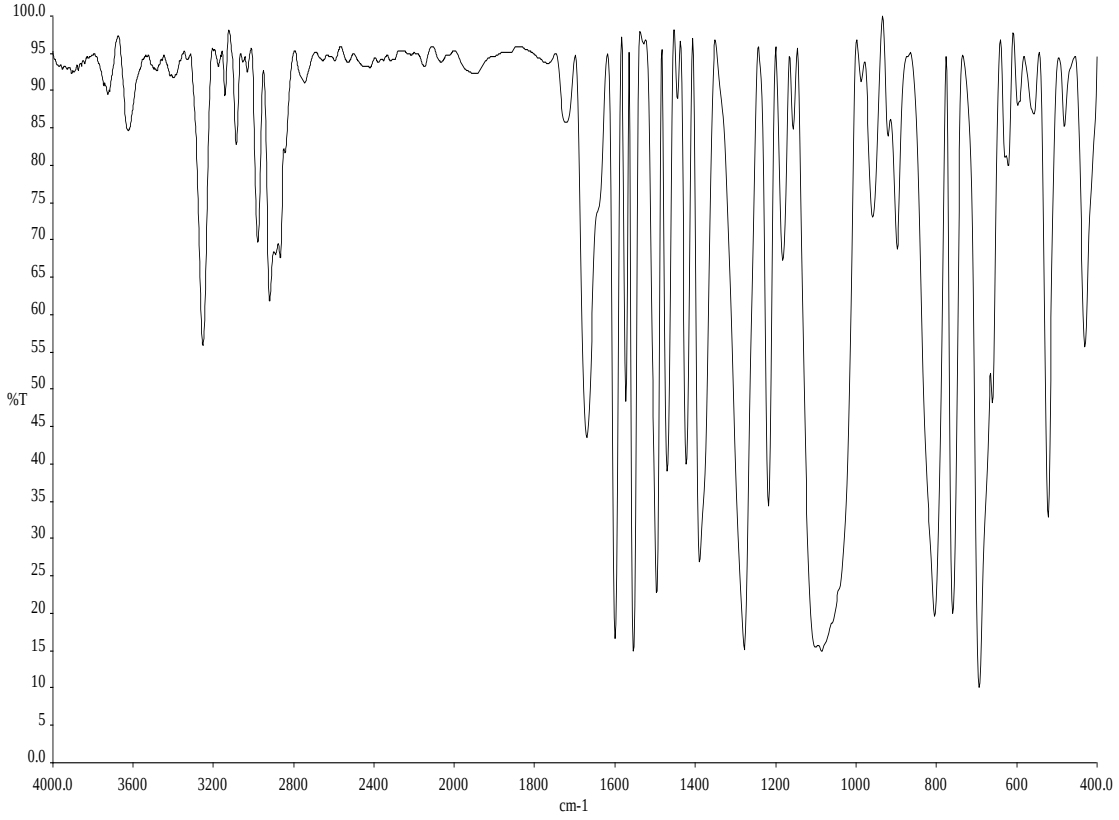

Fig.4.7. IR spectrum of [Cu(bdpab)Br]BF_4 (**4**).

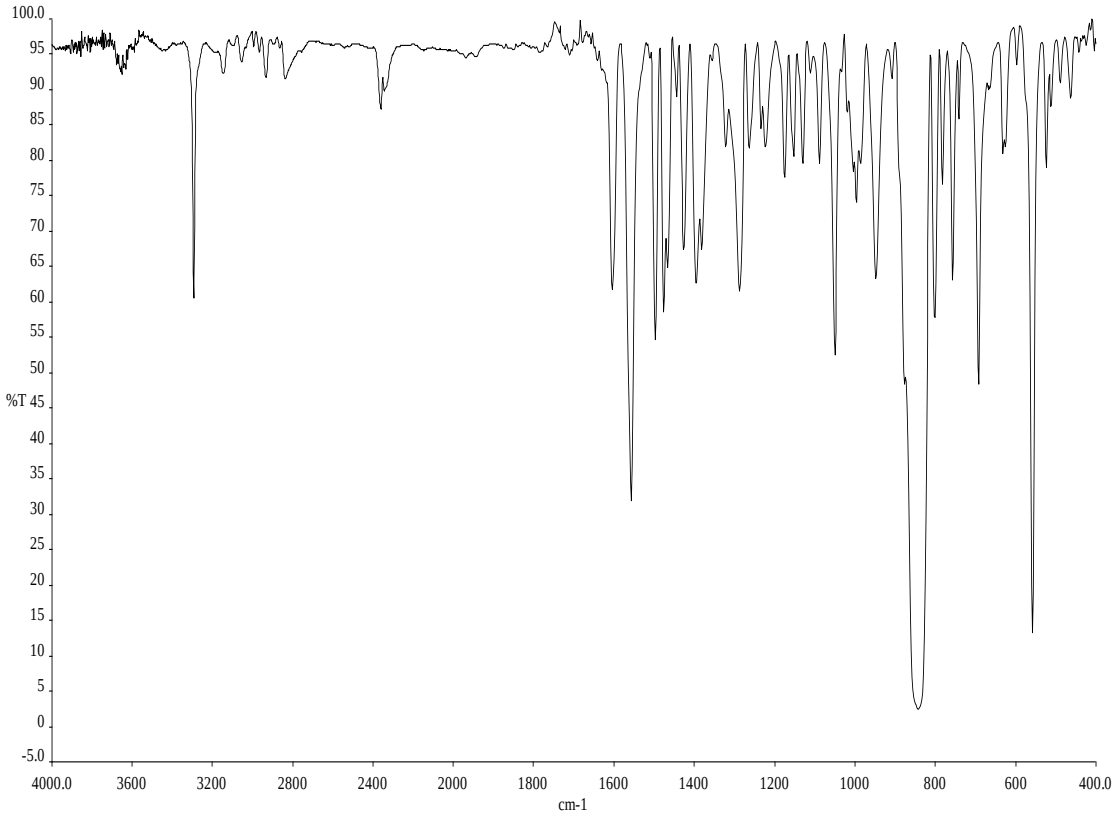

Fig.4.8. IR spectrum of $[Co(bdpab)Cl]_2(PF_6)_2$ (**5**).

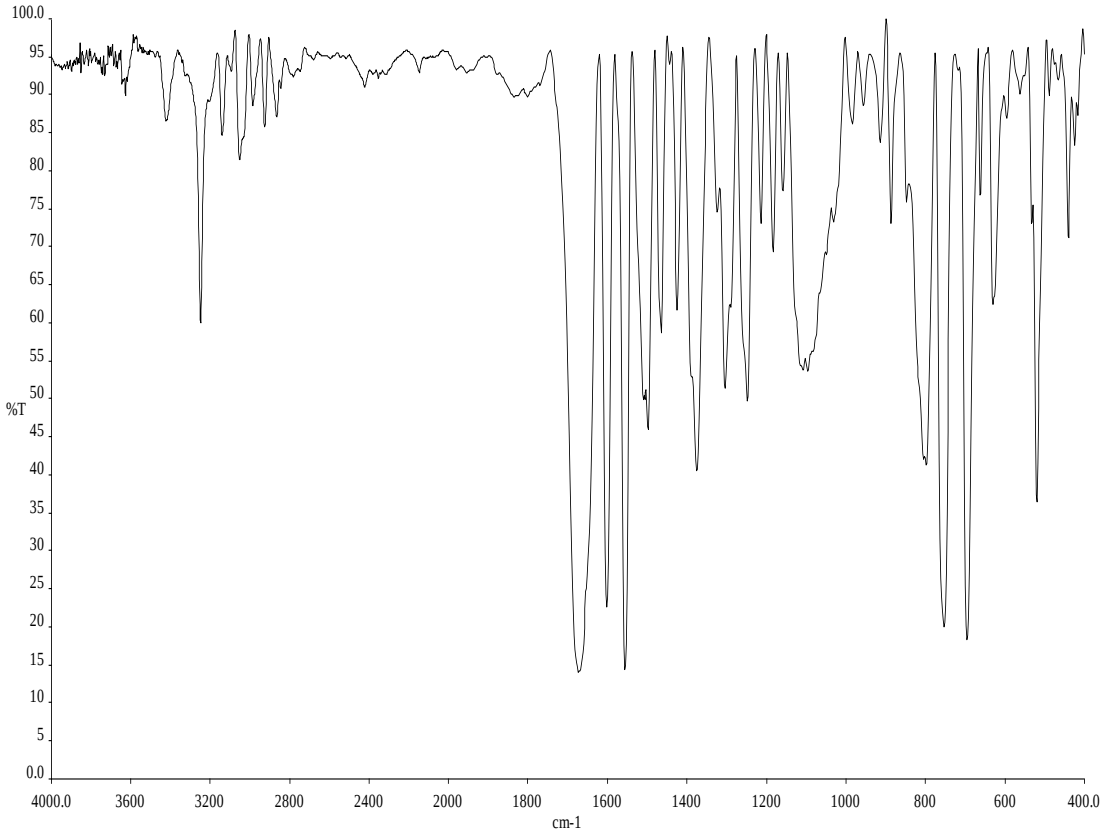

Fig.4.9. IR spectrum of $[Co(bdpab)Cl]_2(BF_4)_2$ (**6**).

4.4.3. UV-Visible spectra, EPR and magnetic data

The UV-Visible spectra of all the complexes **1-6** were recorded in CH_3CN (10^{-3} M) in the range of 200-1100 nm. The high intensity bands appeared at < 400 nm are due to intra ligand n-π* and π-π* charge transfer transition. In the visible region, a broad absorption band was observed at λ>670 nm due to d_{xy}, $d_{yz} \rightarrow d_{x^2-y^2}$ for all copper (II) complexes. This type of spectral feature is typical for Cu(II) complexes with square pyramidal geometry. Generally, trigonal bipyramidal Cu(II) complexes show two spectral bands in the region of 700 -750 nm (due to d_{xy}, $d_{yz} \rightarrow d_{z^2}$) and at 800-870 nm (due to d_{xy}, $d_{x^2-y^2} \rightarrow d_{z^2}$) transition. Absence of spectral band in the two regions in the compounds also support the geometry around copper(II) center is distorted square pyramidal [38-39]. For cobalt(II) complexes, the three absorption bands appeared at 830, ~ 630, ~ 530 nm for complexes **5** and **6** and these are due to d-d transition or ligand field transitions. This type of transitions are generally observed for high spin cobalt(II) complexes.

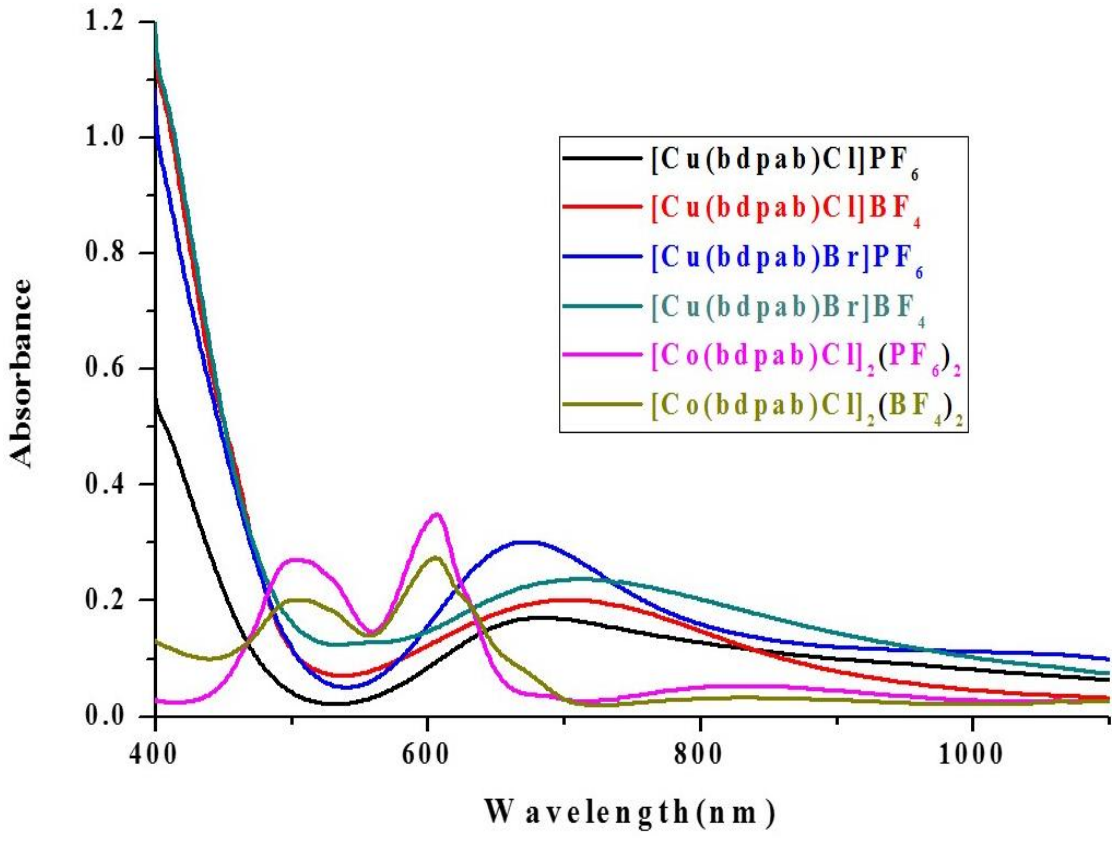

Fig.4.10. Electronic spectra of complexes **1**, **2**, **3**, **4**, **5**, **6** in CH_3CN (10^{-3} M).

The X-band EPR spectra of the complexes **1** and **3** in acetonitrile solution (77 K) show four-line splitting pattern with g_{II} = 2.244 and $g_{\perp}$ = 2.042 for complex **1** and with g_{II} = 2.252 and $g_{\perp}$ = 2.051 for complex **3**, indicating the interaction of the unpaired electron with nuclear spin of the copper(II) nucleus (^{63,65}Cu; I = 3/2). The g_{II} value is greater than $g_{\perp}$, indicating a pseudotetragonal site symmetry of the copper(II) in the complexes.

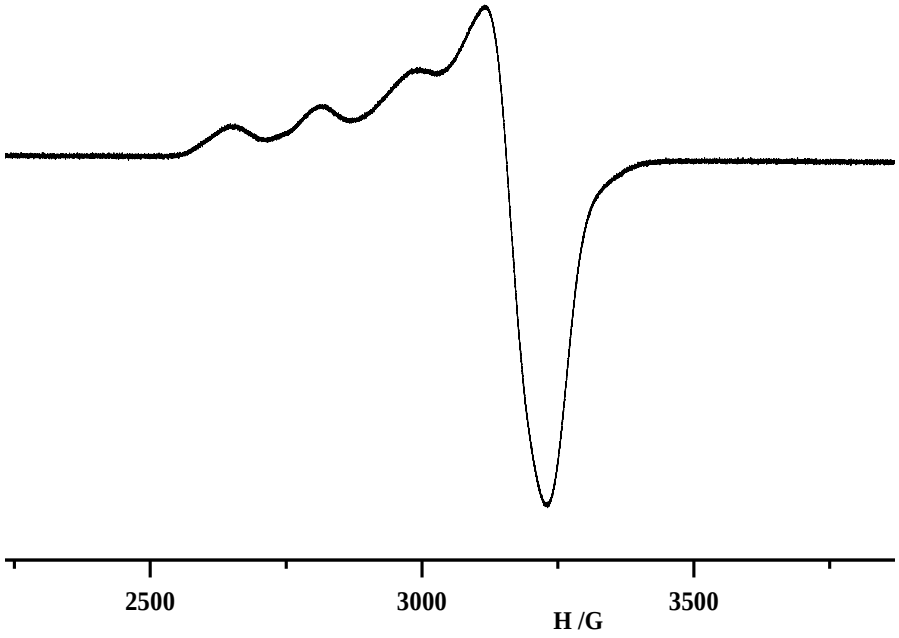

Fig.4.11. X-Band EPR spectrum of complex **1** in DMF solution at 77 K.

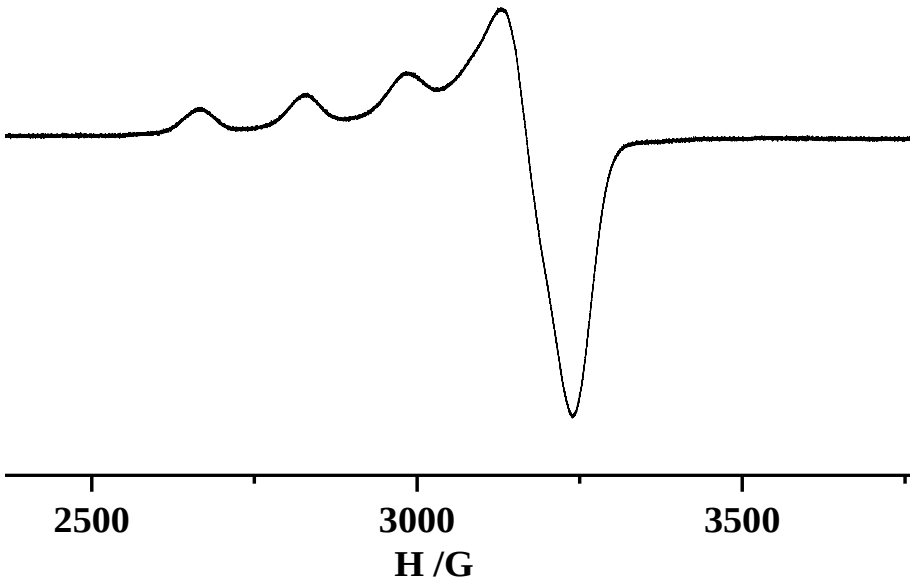

Fig.4.12. X-Band EPR spectrum of complex **3** in DMF solution at 77 K.

Room temperature magnetic susceptibility measurements of powder sample of the complexes show that the complexes have magnetic moments close to their spin only value for Cu(II) complexes (S = 1/2) with μ_{eff} ~ 1.75 BM indicating one electron paramgnetism, for Co(II) complexes (S = 3/2) with μ_{eff} ~ 4.37 BM indicating three electron paramgnetism, respectively. In general, magnetic moment of cobalt(II) complex with tetradentate N_4-coordinate ligand fall in this region [40-41].

4.4.4. Description of Crystal Structures

4.4.4.1. Crystal structures of [Cu(bdpab)X]PF_6 [X= Cl(1), Br(3)]

The structural data show that both complexes **1** and **3** crystalize in the triclinic crystal system with the *P-1* space group and consists of two mononuclear motifs in packing which are further engaged with CH-π and π-π interaction among themselves to give supramolecular 1D structure. ORTEP diagrams with the atom labelling scheme of the monomeric cations $[Cu(bdpab)Cl]^+$ of (**1**) and $[Cu(bdpab)Br]^+$ of (**3**) are shown in Fig.4.13(a) and 4.14(a). A summary of the X-ray crystallographic data and selected bond distance and angles are given in Table. 4.1 and 4.2. In both complexes, the copper(II) center has five coordination- four coordination from nitrogen atoms [N(1), N(2), N(3) and N(6)] of ligand bdpab and the remaining position is occupied by respective halides [Cl(1) or Br(1)]. So the environment around five coordinated copper(II) center can be described as a structure between square-pyramidal (SP) and trigonal–bipyramidal (TBP). Addison et al defined the angular structural index geometric parameter [$\tau = (\beta - \alpha)/60$] (where β and α are the two largest angles of the metal coordination sphere) which is applicable to five co-ordinate structures as an index of the degree of trigonality. The parameter has been used to describe the degree of structural distortion from the SP geometry ($\tau = 0$) to the TBP geometry ($\tau = 1$) [42]. The value of τ are 0.17 and 0.16 for complexes **1** and **3**, respectively, indicating that copper(II) center in both complexes were adopted slightly distorted square pyramidal geometry. In square pyramidal (4+1) geometry, the basal plane formed by two pyrazole nitrogens N(3) and N(6), one tertiary nitrogen N(2) from ligand bdpab and one halide X(1) [X= Cl(1) or Br(1)] and secondary nitrogen atom N(1) from ligand bdpab coordinated axially to copper(II) center at a long distance. For both complexes, the chelate ligand is coordinated in a neutral form in a tetradentate N_4 manner via two pyrazole nitrogen atoms N(3) and N(6), one tertiary nitrogen atom N(2) and one secondary aniline nitrogen atom N(1) forming three five-membered chelate rings.

Table 4.2. Important bond lengths (Å) and bond angels (º) of complexes **1**, **3** and **5**.

Bond lengths (Å)

[Cu(bdpab)Cl]PF_6 (1)		**[Cu(bdpab)Br]PF_6 (3)**		**[Co(bdpab)Cl]$_2$(PF_6)$_2$ (5)**	
Cu(1)-N(3)	1.977(3)	Cu(1)-N(6)	1.983(2)	Co(1)-N(2)	2.2324(17)
Cu(1)-N(6)	1.982(3)	Cu(1)-N(3)	1.988(2)	Co(1)-N(3)	2.1233(17)
Cu(1)-N(2)	2.114(2)	Cu(1)-N(2)	2.123(2)	Co(1)-N(5)	2.1303(17)
Cu(1)-N(1)	2.410(3)	Cu(1)-N(1)	2.391(2)	Co(1)-N(1)	2.2245(18)
Cu(1)-Cl(1)	2.2404(8)	Cu(1)-Br(1)	2.3783(4)	Co(1)-Cl(1)	2.4786(5)
				Co(1)-Cl(1i)	2.4259(5)
				Co(1)-Co(1i)	3.607

Bond angels (º) of complexes **1**, **3** and **5**.

[Cu(bdpab)Cl]PF_6 (1)		**[Cu(bdpab)Br]PF_6 (3)**		**[Co(bdpab)Cl]$_2$(PF_6)$_2$ (5)**	
N(3)-Cu(1)-N(6)	161.24(10)	N(6)-Cu(1)-N(3)	160.82(9)	N(3)-Co(1)-N(2)	77.40(6)
N(3)-Cu(1)-N(2)	79.85(10)	N(6)-Cu(1)-N(2)	79.54(8)	N(5)-Co(1)-N(2)	76.35(6)
N(6)-Cu(1)-N(2)	82.26(10)	N(3)-Cu(1)-N(2)	82.27(8)	N(5)-Co(1)-N(3)	153.71(7)
N(3)-Cu(1)-Cl(1)	97.40(8)	N(6)-Cu(1)-Br(1)	96.98(6)	N(1)-Co(1)-N(2)	80.10(6)
N(6)-Cu(1)-Cl(1)	99.46(8)	N(3)-Cu(1)-Br(1)	100.04(6)	N(1)-Co(1)-N(3)	89.35(7)
N(2)-Cu(1)-Cl(1)	171.25(7)	N(2)-Cu(1)-Br(1)	170.59(6)	N(1)-Co(1)-N(5)	87.56(7)
N(3)-Cu(1)-N(1)	92.27(10)	N(6)-Cu(1)-N(1)	92.09(9)	Cl(1i)-Co(1)-N(2)	178.03(4)
N(6)-Cu(1)-N(1)	90.54(10)	N(3)-Cu(1)-N(1)	91.21(8)	Cl(1)-Co(1)-N(2)	95.77(4)
N(2)-Cu(1)-N(1)	81.22(9)	N(2)-Cu(1)-N(1)	81.56(8)	Cl(1i)-Co(1)-N(3)	104.24(5)
Cl(1)-Cu(1)-N(1)	107.27(7)	Br(1)-Cu(1)-N(1)	107.41(5)	Cl(1)-Co(1)-N(3)	91.34(5)
				Cl(1)-Co(1)-N(5)	89.89(5)
				Cl(1i)-Co(1)-N(5)	102.04(5)
				Cl(1)-Co(1)-N(1)	175.56(5)
				Cl(1i)-Co(1)-N(1)	98.76(5)

For complex **1**, equatorial bond distances of Cu-N(2) [2.114(2) Å], Cu(1)-N(3) [1.977(3) Å], Cu(1)-N(6) [1.982(3) Å] and Cu(1)-Cl(1) [2.2404(8)Å] are not same and axial position is occupied by secondary nitrogen N(1) with long Cu-N(1) [2.410(3)Å] distance. Deviations of coordinating atoms N(2), N(3), N(6) and Cl(1) from the mean plane are 0.049, 0.0076, 0.009 and 0.048 Å, respectively. In this square pyramidal structure, the copper(II) is slightly displaced 0.112 Å out of this mean square plane towards the secondary amine nitrogen of ligand bdpab. The chelate bite angles for three five membered chelate rings, N(1)–Cu(1)–N(2), N(2)–Cu(1)–N(3) and N(2)–Cu(1)–N(6) are 171.25(7)º, 79.85(10)º and 82.26(10)º, respectively. The bond angles and distances are comparable to previously reported chloride and N_4-coordinated tripodal ligand containing copper(II) complexes [43-44].

The shortest Cu----Cu separation is 3.893 Å and the Cu(1)-----Cl(1) [2-x, 1-y, 2-z] separation is 3.120 Å, thus formation of supramolecular dimer is observed [Fig.4.13(b)]. Two molecules in a unit cell are attached together through π….π stacking between the two phenyl rings of two nearest ligand bdpab with distance between the two centroids Cg(1)-Cg(2) is 3.958 Å and C-H….π interactions between one hydrogen atom of $–CH_3$ group attached with pyrazole ring of one ligand and nearest pyrazole ring of the another ligand with distance C20-H20B-Cg(3) is 2.872 Å and thus forming 1D chain along c-axes [Fig.4.13(c)] [45-46].

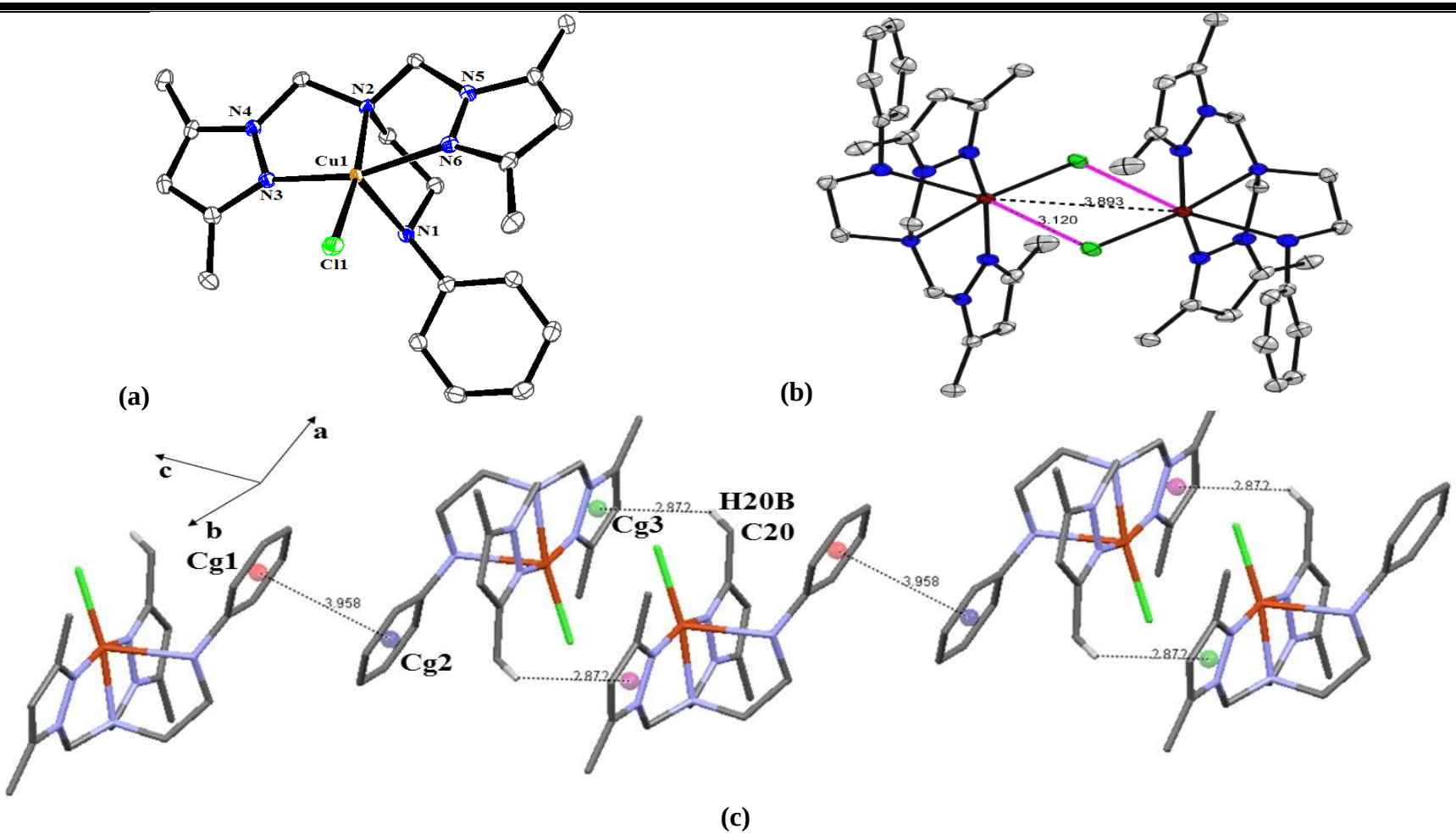

Fig.4.13(a). ORTEP diagram depicting the cationic part of the complex [Cu(bdpab)Cl]PF_6 (**1**) with atom numbering scheme (40% probability factor for the thermal ellipsoids). **(b).** Perspective view of the supra molecular dimer $[\{Cu(bdpab)Cl\}]^{2+}$ of **1**. **(c).** Intermolecular interactions of complex**1.**

For complex **3,** the two equatorial bond distances of Cu(1)-N(3) [1.988(2) Å], Cu(1)-N(6) [1.983(2) Å] are shorter than Cu(1)-Br(1) [2.3783(4) Å] or Cu-N(2) [2.123(2) Å] and the apical position is occupied by secondary nitrogen N(1) with long Cu-N(1) [2.391(2)Å] distance. Deviations of coordinating atoms N(2), N(3), N(6) and Br(1) from the mean plane are 0.055, 0.010, 0.007 and 0.051 Å, respectively. For a square pyramidal structure, the copper(II) is displaced by 0.112 Å out of this mean square plane towards the secondary amine nitrogen of ligand bdpab. The chelate bite angles for three five membered chelate rings, N(1)–Cu(1)–N(2), N(2)–Cu(1)–N(3) and N(2)–Cu(1)–N(6) are 171.25(7), 79.85(10) and 82.26(10)º respectively. The bond angles and distances are comparable with previously reported copper(II) bromide complex containing tripodal ligand [47].

Two molecules in a unit cell are attached together through π….π stacking between the two phenyl rings of two nearest ligand bdpab with distance between two centroids [Cg(1)-Cg(2)] is 4.027 Å and C-H….π interactions between one hydrogen atom of $–CH_3$ group attached with pyrazole ring and pyrazole ring of the nearest ligand with distance C11-H11c-Cg(3) is 2.936 Å and forming 1D chain along c-axes [Fig.4.14(b)] [45-46].

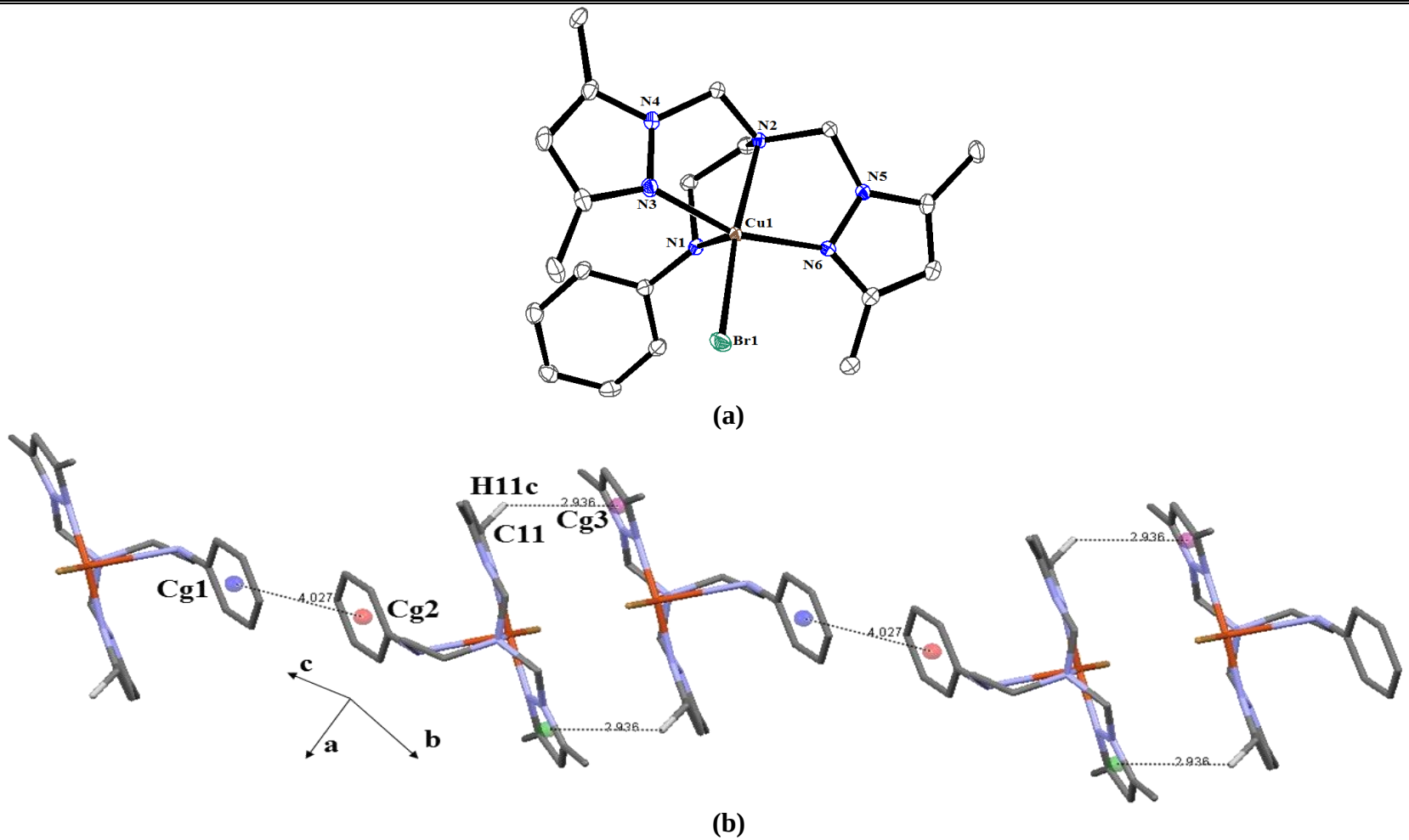

Fig.4.14 (a). ORTEP diagram depicting the cationic part of the complex [Cu(bdpab)Br]PF_6 (**3**) with atom numbering scheme (40% probability factor for the thermal ellipsoids). **(b).** Intermolecular interactions of complex **3.**

4.4.4.2. Crystal structure of $[Co(bdpab)(\mu\text{-}Cl)]_2(PF_6)_2$ (5)

The X-ray study revealed that dark pink crystal of complex **5** crystallize in triclinic system with P-1 space group [a = 9.6899(3), b = 10.8074(5), c = 13.1823(5) Å] contains one dimeric $[Co(bdpab)(\mu\text{-}Cl)]^{+2}$ cation. An ORTEP diagram of the dimeric cation with atom labeling is shown in Fig.4.15(a). Selected bond lengths and angles are given in Table 4.2. Crystal structure of the complex shows that the complex consists of double choride bridged dimer in which bridging Co_2Cl_2 is planar due to the presence of crystallographic inversion center in the middle of dimer.

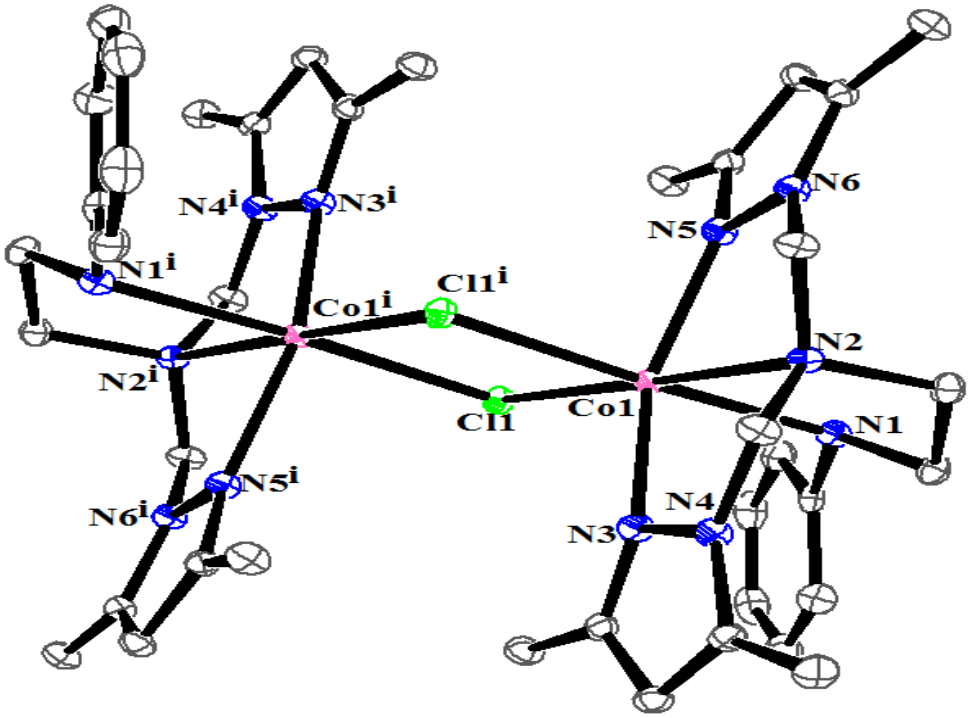

Fig.4.15(a). ORTEP diagram depicting the cationic part of the complex $[Co(bdpab)(\mu\text{-}Cl)]_2(PF_6)_2$ (**5**) with atom numbering scheme (40% probability factor for the thermal ellipsoids).

In dimeric cation, both cobalt(II) centers are six coordinated and the geometry around Co(II) centres can be described as distorted octahedral. Each cobalt atom is bonded to tetradentate ligand bdpab and remaining coordination sites are occupied by two bridging chloride ions. Structural data shows that equatorial plane is occupied by three potential nitrogen donors N(2), N(3), N(5) and Cl(1i) from ligand and the remaining two axial positions are secured by one secondary nitrogen atom N(1) of the ligand and one chloride ion Cl(1). Ligand bdpab forms three ligand-metal-ligand

chelate ring with bite angles varying between 76.35(6)º and 80.10(6)º and the rings are puckered so that the torsion angles of N(5)-N(6)-C(10)-N(2), N(2)-C(9)-N(4)-N(3) and N(2)-C(8)-C(7)-N(1) are 38.31º, 42.12º and 54.76º, respectively [48-49].

In complex **5,** the [Co(μ-Cl)$_2$Co] motif has been found in number of crystallographically characterized complexes and this motif is asymmetric because of two Co-Cl bond lengths are 2.4786(5) and 2.4259(5)Å and the Co(1)-Cl(1)-Co(1i) bridging angle is 94.67º. The intra dimer cobalt-cobalt distance is 3.607 Å. The Co-Cl and Co…Co bond length values are comparable with earlier reported chloride bridged cobalt complex with similar structure [44].

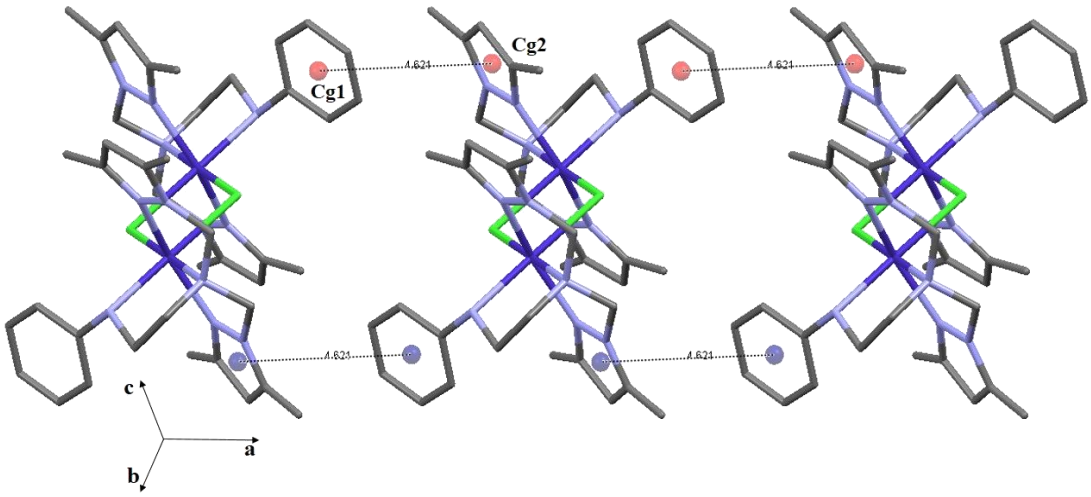

Fig.4.15(b). Intermolecular interaction of complex **5.**

In complex **5,** two binuclear molecules in unit cell are assembled by means of intermolecular face-to-face π-π interaction between phenyl ring and pyrazole ring of two nearest molecules with the centroid-centroid [Cg(1)-Cg(2)] distance is 4.260 Å [Fig.4.15(b)] and the dihedral angle between them is 18.89º indicating a significant intermolecular face-to-face π---π stacking interaction. The π-π interaction has formed 1D linear polymer along a- axis [45].

4.4.5. Antimicrobial activity

The Cu(II) and Co(II) complexes with the resolved structure viz. **1**, **3** and **5** and their ligands were studied for their antimicrobial activity against *Bacillus subtilis, Streptococcus aureus, Escherichia Coli* and *Pseudomonas aeruginosa* as shown in Table 4.3. No inhibition was observed in the negative control plate and strong inhibition in the presence of chloramphenicol proved the susceptibility of microorganisms to antimicrobial agents.

Table 4.3. IC_{50} and MIC activity data of the bdpab ligand, salts and complexes **1**, **3** and **5**.

Compound	**IC_{50} value**	**MIC value in mM**			
		S. aureus	***B. Subtilis***	***E. coli***	***P. aeruginosa***
$CuCl_2.2H_2O$	408.3	>10	>10	10	>10
$CuBr_2.4H_2O$	314.2	>10	>10	>10	>10
$CoCl_2.6H_2O$	3119.18	10	10	10	10
bdpab	601.028	>10	>10	>10	10
$[Cu(bdpab)Cl]PF_6$ (1)	214.69	5	5	10	>10
$[Cu(bdpab)Br]PF_6$ (3)	68.34	10	10	5	10
$[Co(bdpab)Cl]_2(PF_6)_2$ (5)	1089.8	5	5	10	10

Complexes **1** and **5** showed highest activity against gram positive microorganism with MIC of 5 mM against both *Bacillus subtilus* and *Streptococcus aureus*. In case of gram negative microorganisms, complex **3** displayed highest antimicrobial activity against *Escherichia coli* with MIC of 5 mM. Complex **3** and **5** equally inhibited *Pseudomonas aeruginosa* with MIC of 10 mM. Antimicrobial activity of cobalt(II) complex **5** was considerably consistent than copper(II) complexes **1** and **3**. A marked increase in the antimicrobial activity was exhibited on

co-ordination of the metal ions with the ligand i.e. after complexation. The enhancement of the activity can be attributed to the presence of metal ions which influence the solubility, conductivity and dipole moment of the complexes which could be the significant factors responsible for increasing the penetration of the molecules into bacterial cell wall, effectively targeting the bacterial machinery by various mechanisms [50]. The antimicrobial activity data shows the copper(II) complexes with aromatic substituent bdpab ligand have higher activity than the previously reported similar complexes with N_4-coordinate pyrazolyl ligand dbdmp with diethyl substituents [51-52].

4.4.6. Anti-proliferative activities of Copper and Cobalt salts and its complexes.

The anti-proliferative activity of free ligand, copper and cobalt salts and their complexes were investigated against A549 lung carcinoma cancer cells. In the present study, all three salts and their complexes showed cytotoxicity. It was found that $[Cu(bdpab)Cl]PF_6$ and $[Cu(bdpab)Br]PF_6$ complexes showed maximum cytotoxicity compared to other complexes reported here and their respective salts [Fig.4.16]. IC_{50} value for the salts and their complexes $CuCl_2.2H_2O$, $CuBr_2.4H_2O$, $CoCl_2.6H_2O$, $[Cu(bdpab)Cl]PF_6$, $[Cu(bdpab)Br]PF_6$, $[Co(bdpab)Cl]_2(PF_6)_2$ and bdpab are 408.3, 314.2, 3119.18, 214.69, 68.34, 1089.8 and 601.028 μg/ml respectively. Metal salts are highly toxic and the ligand is nontoxic but showed potent cytotoxicity following its chelation with metal ions. Hence it can be concluded that the cytotoxic activity obtained with complexes are better than corresponding metal salts and among the synthesized complexes, $[Cu(bdpab)Br]PF_6$ complex has best cytotoxic activity against human lung carcinoma cells.

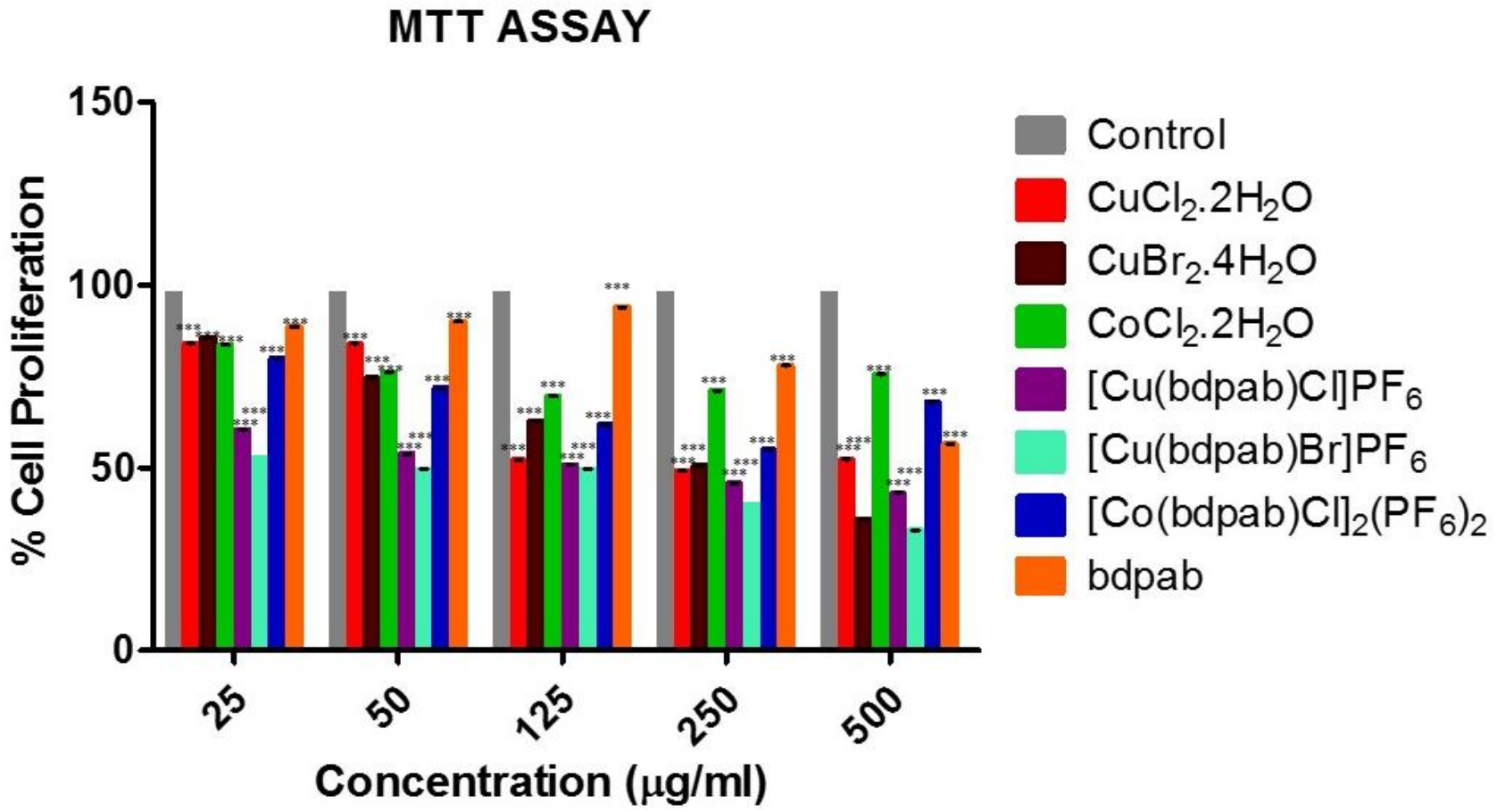

Fig.4.16. Effect of Complexes exposed to A549 cells on cell viability. Data expressed as mean ± S.E.M. for n = 3. ***P < 0.001.

4.4.7. Cleavage experiment

In order to find out DNA cleavage activity of the synthetized compounds, the interaction of plasmid pBS KS(+) with the compounds in the presence of H_2O_2 was studied. The gel picture showing the cleavage of plasmid DNA by the complexes is depicted in [Fig.4.17]. Thick bands were observed in the controls viz. untreated plasmid, plasmid with H_2O_2 only and plasmid with complex (50μM) only in lane1, lane 2 and lane 3 respectively. This suggested that the plasmid was intact without treatment and H_2O_2 and the complexes alone had no effect on the plasmid. The disappearance of the DNA bands after gel electrophoresis very clearly revealed that the complex **1** and **3** effectively cleaved the DNA even at the low concentration of 10 μM. In case of complex **5,** the difference in the band thickness in controls and the treated samples was not much significant. The cleavage is thought to occur by the attack of free oxygen radicals produced by H_2O_2 on the DNA exposed after the treatment with the complexes [53]. On the basis of the results it is evident that the complex **1** and **5** are effective DNA cleavage agents. The usage of DNA cleavage compounds range from cleavage at specific sites and complete digestion in molecular biology to targeted cleavage of cancer cell's DNA in chemotherapy and arresting the growth of pathogenic bacteria and viruses [54-56]. The copper complexes are being explored extensively for their use as chemical nucleases because they possess biologically accessible redox potential and relatively high nucleobase affinity [57-58].

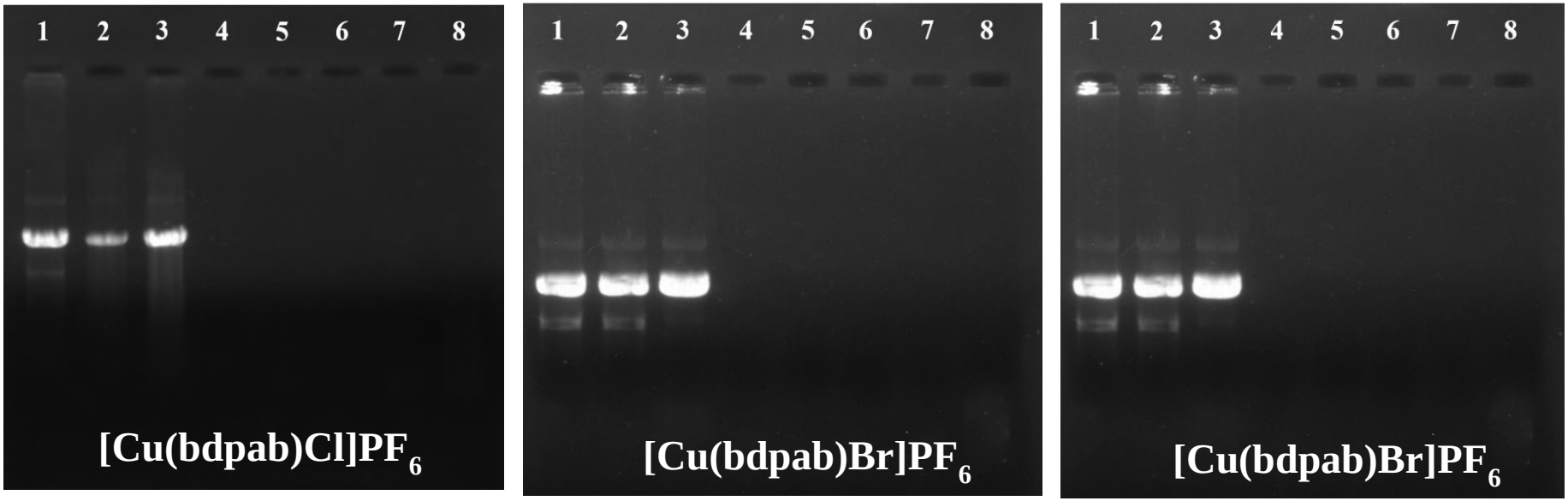

Fig.4.17. Cleavage of DNA(pbs KS(+)) induced by complexes: Lane 1, untreated DNA; lane 2, plasmid DNA + 3 µl H_2O_2; lane 3, plasmid DNA + 50 µM complex; lane 4, plasmid DNA + 10 µM complex + 3 µl H_2O_2; lane 5, plasmid DNA + 20 µM complex + 3 µl H_2O_2; lane 6, plasmid DNA + 30 µM complex + 3 µl H_2O_2; lane 7, plasmid DNA + 40 µM complex + 3 µl H_2O_2; lane 8, plasmid DNA + 50 µM complex + 3 µl H_2O_2, respectively.

4.5. Conclusions

A new N_4-coordinated tripodal ligand *N*,*N*-bis(3,5-dimethyl-*1H*-pyrazol-1-yl)methyl-N_2-phenylethane-1,2-diamine (bdpab) and a series of Cu(II)/Co(II) halide complexes with ligand bdpab have been synthesized and characterized. Structural data show mononuclear copper(II) complexes are five coordinated with square pyramidal geometry and binuclear cobalt(II) complexes are six coordinated with octahedral geometry. In cobalt(II) complex, two $[Co(bdpab)Cl]^+$ units are linked by two (μ-Cl) bridges. Antimicrobial studies showed that all the tested complexes possess antimicrobial activity with complexes **1** and **5** are more effective against gram positive bacteria and complex **3** is more effective against gram negative bacteria. The complexes have complete DNA cleaving ability in presence of H_2O_2 even at very low concentrations. Cytotoxic activity of the complexes show copper complexes have cytotoxic activity and among the copper complexes, $[Cu(bdpab)Br]PF_6$ has highest activity. The molar conductivity values in acetonitrile of the mono- and dinuclear complexes are supporting 1:1 electrolyte. So the bioactivity data indicates that the dinuclear cobalt(II) complex disassembles in solution to render the corresponding mononuclear species which are responsible for the bioactivities.

4.6. References

1. E.R Jamieson, S.J. Lippard., Chem. Rev. 99 (1999) 2467.
2. L. Kelland, Nat. Rev. Cancer 7 (2007) 573.
3. C. He, C. Poon, C. Chan, S. D. Yamada, W. Lin, J. Am. Chem. Soc.138 (2016) 6010.
4. R Lincoln., Kohler, S. Monro, H. Yin, M. Stephenson, R. Zong, A. Chouai, C.Dorsey, R. Hennigar, R.P. Thummel, S.A. McFarland, J. Am. Chem. Soc.135 (2013) 17161.
5. E.I. Solomon, P. Chen, M. Metz, S.K. Lee, A.E. Palmer, Agnew. Chem. Int. Ed. 40 (2001) 4570
6. C. Santini, M. Pellei, V. Gandin, M. Porchia, F. Tisato, C. Marzano, Chem. Rev. 114 (2014) 815.
7. R. Ruiz, B. Garcia, J. Garcia-Tojal, N. Busto, S. Ibeas, J.M. Leal, C. Martins, J. Gaspar, J. Borras, R. Gil-Garcia, M.G. Alvarez, J. Biol. Inorg. Chem. 15 (2010) 515.
8. M.J. Wiester, P.A. Ulmann, C.A. Mirkin, Angew, Chem. Int. Ed. 50 (2011) 114.
9. F. Mancin, P. Scrimin, P. Tecilla, U. Tonellato, Chem. Commun. (2005) 2540.
10. X.-Q. Zhou, Q. Sun, L. Jiang, S.-T. Li, W.Gu, J.-L. Tian, X. Liu, S.-P. Yan, Dalton Trans. 44 (2015) 9516.
11. M. Alagesan, N.S.P. Bhuvanesh, N. Dharmaraj, Dalton Trans. 42 (2013) 7210.
12. S. Bhattacharyya, A. Sarkar, S.K. Dey, G.P. Jose, A. Mukherjee, T.K. Sengupta, Dalton Trans. 42 (2013) 11709.
13. L. Liu, G.M. Zhang, R.G. Zhu, Y.H. Liu, H.M. Yao, Z.B. Han, RSC Adv. 4 (2014) 46639.
14. P.R. Reddy, A. Shilpa, N. Raju, P. Raghavaiah, J. Inorg. Biochem. 105 (2011) 1603.
15. R. Ren, P. Yang, W.J. Zheng, Z.C. Hua, Inorg. Chem. 39 (2000) 5454.
16. S. Anbu, M. Kandaswamy, S. Kamalraj, J. Muthumarry, B. Varghese, Dalton Trans. 40 (2011) 7310.
17. A. Prisecaru, V. Mckee, O. Howe, G. Rochford, M. McCann, J. Colleran, M. Pour, N. Barron, N. Gathergood, A. Kellett, J. Med. Chem. 56 (2013) 8599.
18. S. Sathiyaraj, K. Sampath, G. Raja, R.J. Butcher, S.K. Gupta, C.J.

Balakrishnan, Inorg. Chim. Acta 406 (2013) 44.

19. C.H. Ng, W.S. Wang, K.V. Chong, Y.F. Win, K.E. Neo, Dalton Trans. 42 (2013) 10233.
20. A.K. Patra, T. Bhowmick, S. Ramakumar, A.R. Chakravarty, Inorg. Chem. 46 (2007) 9030.
21. C. Fernandes, G.L. Parrilha, J.A. Lessa, L.J.M. Santiago, M.M. Kanashiro, F. S. Boniolo, A.J. Bortoluzzi, N.V. Vugman, M.H. Herbst, A. Horn Jr, Inorg. Chim. Acta 359 (2006) 3167.
22. K. Ghosh, P. Kumar, V. Mohan, U.P. Singh, S. Kasiri, S.S. Mandal, Inorg. Chem. 51 (2012) 3343.
23. T.W. Failes, C. Cullinane, C.I. Diakos, N. Yamamoto, J.G. Lyons, T.W. Hambley, Chem. Eur. J. 13 (2007) 2974.
24. K. Miyoshi, H. Tanaka,E. Kimura, S. Tsuboyama, S. Murata, H. Shimizu, K. Ishizu, Inorg. Chim. Acta 78 (1983) 23.
25. H. Gopinathan, N. Komathi, M.N. Arumugham, Inorg. Chim. Acta 416 (2014) 93.
26. E.V. Rybak-Akimova, A.Y. Nazarenko, L. Chen, P.W. Krieger, A.M. Herrera, V.V. Tarasov, P.D. Robinson, Inorg. Chim. Acta 324 (2001) 1.
27. J.-R.Guo, Q.-Q. Chen, C.W.-K. Lam, W. Zhang, Biol. Res. 48 (2015) 40.
28. H.C. Bimboim, J. Doly, Nucl. Acids Res. 7 (1979) 1513
29. J. Marmur, J. mol. Biol. 3 (1961) 208.
30. M.E. Reichmann, S.A. Rice, C.A. Thomas, P. Doty, J. Am. Chem. Soc. 76 (1954) 3047.
31. Agilent, CrysAlis PRO. Agilent Technologies UK Ltd, Yarnton, England, (2011).
32. G.M. Sheldrick, SAINT, 5.1 ed. Siemens Industrial Automation Inc., Madison, WI, (1995)
33. G.M. Sheldrick. SHELXL-97: Program for Crystal Structure Refinement, University of Gottingen, Gottingen, (1997).
34. L.J. Farrugia, J. Appl. Cryst. 32 (1999) 837.
35. L.J. Farrugia, J. Appl. Cryst. 30 (1997) 565.
36. W.J. Geary, Coord. Chem. Rev.7 (1971) 81.
37. K. Nakamoto, Infrared and Raman Spectra of Inorganic and Coordination

Compounds, 3rdedn. Wiley Interscience, New York, (1978).

38. U. Mukhopadhayay, I. Bernal, S.S. Massoud, F.A. Mautner, Inorg. Chim. Acta 357 (2004) 3873.
39. S.S. Massoud, F.A Mautner, M.A.M. Abu-Youssef, N.M. Shuaib, Polyhedron 18 (1999) 2061.
40. B. Chakraborty, T.K. Paine, Inorg. Chim. Acta 378 (2011) 231.
41. J. Matsumoto, T. Suzuki, Y. Kajita, H. Masuda, Dalton Trans. 41 (2012) 4107.
42. A.W. Addison, T.N. Rao, J.Reedijk, J.V. Rijn, G.C. Verschoor, J. Chem. Soc. Dalton Trans. (1984) 1349.
43 Y. Funasako, M. Nosho, T. Mochida, Dalton Trans. 42 (2013) 10138.
44. R. Herchel, Z. Dvorak, Z. Travnicek, M. Mikuriya, F.R. Louka, F.A. Mautner, S.S. Massoud, Inorg. Chim. Acta 451 (2016) 102.
45. M.H. Sadhu, S.B. Kumar Polyhedron 123 (2017) 419.
46. G. Aragay, D. Hernandez, B. Verdejo, E.C. Escudero-Adan, M. Martinez, P. Ballester, Molecules 20 (2015) 16672.
47. T.E. Patten, M.M. Olmstead, C. Troeltzsch, Inorg. Chim. Acta 361 (2008) 365.
48. C.J. Davies, G.A. Solan, J. Fawcett, Polyhedron 23 (2004) 3105.
49. S.B. Kumar, M. Zala, A. Solanki, M. Rangrez, P. Parikh, E. Suresh, Polyhedron 36 (2012) 15.
50. Z.H. Chohan, H. Pervez, A. Rauf, A. Scozzafava, C.T. Supuran, J. Enzyme Inhib. Med. Chem. 17 (2) (2002) 117.
51. A. Solanki, S.B. Kumar, A.A. Doshi, C. RatnaPrabha, Polyhedron 63 (2013) 147.
52. A. Solanki, M.H. Sadhu, S. Patel, R. Devkar, S.B. Kumar, Polyhedron 102 (2015) 267.
53. S. Tang, Y. Feng, Z. Xu, Y. Yang, D. Wang, Asian J. Chem. 25 (2013) 9237.
54. M. Pitie, C.J. Burrows, B. Meunier, Nucl. Acids Res. 28 (2000) 4856.
55. X. Lu, K. Zhu, M. Zhang, Liu, H. Kang, J.J. Biochem. Biophy. Methods, 52 (2002) 189.
56. K.M. Vyas, R.G. Joshi, R.N. Jadeja, C. RatnaPrabha, V.K. Gupta, Spectrochim Acta Part A 84 (2011) 256.
57. W.K. Pogozelski, T.D. Tullius, Chem. Rev. 98 (1998) 1089.
58. C.J. Burrows, J.G. Muller, Chem. Rev. 98(3) (1998) 1109.